UNIVERSITY OF TWENTE.

Faculty of Electrical Engineering, Mathematics & Computer Science

Antenna system design for OLFAR's inter-satellite link

Teodoro J. Willink Castro

M.Sc. Thesis
October 2012

Supervisors:
prof. dr. W. G. Scanlon
dr. ir. M. J. Bentum
dr. ir. A. Meijerink
dr. ing. E. A. M. Klumperink
A. Budianu, M.Sc.

Telecommunication Engineering Group
Faculty of Electrical Engineering,
Mathematics and Computer Science
University of Twente
P.O. Box 217
7500 AE Enschede
The Netherlands

Acknowledgements

The experience of living more than two years in the Netherlands with the excuse of pursuing a master's degree is definitely a life-changing, eye-opening, mind-blowing experience, especially for a Costa Rican who has lived all his life in the other side of the world. This work in some way represents this experience, with all the discoveries, losses, adventures and lessons that it has brought.

Working in the inter-satellite communications layer of the OLFAR project with Alex, advised and supervised by Mark (Dr. Bentum) and Arjan (Dr. Meijerink) has certainly smashed my expectations of working in an academic environment in a Dutch university. Moreover, participating in three papers and an international conference has certainly made this master thesis project one of the most challenging and amazing projects I have been involved in. With all the social, cultural and sports activities going on around it, time has simply run short too fast.

I want to dedicate a short part of this document to acknowledge the unconditional support of my family and friends, who have been with me during this crazy adventure, for some even despite of a considerable geographical distance. My mom, my sister, my grandparents and my dad have aways been close to me and definitely are the main reason of me writing this here, now. However, my friends are also an important part of this. Either if they are old friends or friends that feel like old, they all deserve a space here (although I may not include a list).

Finally, the advice and patience from Alex, Mark and Arjan, as well as the warm support from the people from the University of Costa Rica and the University of Twente, is the direct cause of this document, with all that it means.

After all this, all I can say is *thank you*... or *muchas gracias*... or *dankjewel*.

- Teo

Summary

Initiatives to perform space-based radio astronomy below 30 MHz have emerged recently, since novel technological developments have increased their feasibility. The Orbiting Low-Frequency Antennas for Radio Astronomy (OLFAR) project, one of these initiatives, aims to use a swarm of nano-satellites to implement a radio interferometric array in space to observe celestial radiation with frequencies in the range of 0.3 MHz to 30 MHz.

For its astronomical tasks, OLFAR requires that every satellite is able to establish a high-data-rate radio link with all the others. The inter-satellite communications subsystem of each satellite consists in a data distribution strategy, the coding, modulation and multiple access schemes and an antenna system, which is addressed in this work.

The antenna system capacity requirements are influenced by the data rate generated by the astronomical observations, as well as the configuration of the data distribution strategy and the communication schemes. Moreover, the antenna system design must also consider the spatial configuration of the interferometric array, since it determines the possible link directions. Additionally, the physical dimensions of the nano-satellites impose important restrictions in available area for the inter-satellite link (ISL) antennas and the transmission power. From all these, we identify the antenna system's requirements and limitations: it must provide enough gain for any link direction given the available area constraint.

To meet these, we present a proposal that consists of four aspects: an antenna configuration, a control scheme, the relevant antenna characteristics and the transceiver architecture possibilities. Six antennas, one on each face of the nano-satellite, make up the proposed antenna configuration. The proposed control scheme is a tailored beamforming algorithm that maxmimizes the antenna system gain for any link direction. The relevant individual antenna characteristics include bandwidth, radiation pattern, polarization, impedance and efficiency. Moreover, a discussion on antenna implementation alternatives for different ISL frequencies is also presented. Finally, digital baseband control is proposed to be used in the transceiver, despite of the additional hardware that it may require.

To validate this proposal, we developed an analytical model and an experimental evaluation platform, which we use to evaluate the performance of the proposed antenna system. The obtained results show that it is possible to obtain the required performance theoretically, although in practice it may not be totally achievable.

We conclude that the proposal meets the identified requirements and limitations with an efficient solution, at the expense of high system complexity. However, the proposed design is flexible enough to consider simpler implementations if the requirements are loosened.

We recommend that further work is carried out towards a careful design of the individual antennas and the integrated transceiver, since they can provide useful insight on their achievable performance and requirements.

Contents

Chapter 1

Introduction

The rapid development of radio astronomy—the study of celestial radiation at radio frequencies—in the last decades has contributed significantly to our understanding of the formation and evolution of the universe. With the advance of technology, improvements in scientific instruments and techniques have allowed critical breakthroughs in the study of astronomical objects and phenomena in the radio-frequency (RF) range. Novel projects under research and development promise to continue this trend, reaching for unexplored bounds and proposing new challenges.

The Orbiting Low-Frequency Antennas for Radio Astronomy (OLFAR) project is a modern initative to perform low-frequency radio astronomy from space, which aims to provide significant scientific contributions but also imposes considerable engineering challenges. This work presents the results of the design process of an antenna system for inter-satellite communications in OLFAR.

1.1 Framework and motivation

As a radio astronomy project, OLFAR is highly motivated by its scientific drivers. This work shares this motivation related to low-frequency radio astronomy, but is also propelled by the challenging requirements that the concept presents, specially for inter-satellite communications.

1.1.1 Radio astronomy

Since its origin in 1932 [1], radio astronomy has presented substantial scientific contributions that range from the observation of galaxies and quasars (in the radio-frequency range) [2] to the discovery of cosmic microwave background radiation [3]. Thus, radio astronomy is regarded nowadays as a fundamental tool for the study of the universe astrophysics [4].

An important motive for the success of radio astronomy is the favorable conditions provided by Earth's atmosphere to observe celestial radio waves. The atmosphere exhibits a highly transparent window for wavelengths between 1 cm and 10 m (i.e. for frequencies between 30 MHz and 30 GHz) [5], along with several other (smaller) windows for observation of millimeter-length radio waves [6]. However, radiation with wavelengths above 10 m experiences severe ionospheric distortions [7] and high levels of man-made radio-frequency interference (RFI) [8], which considerably limit Earth-based observations. Figure 1.1 shows the atmospheric electromagnetic (EM) opacity for different wavelengths, from where the mentioned observation windows can be appreciated.

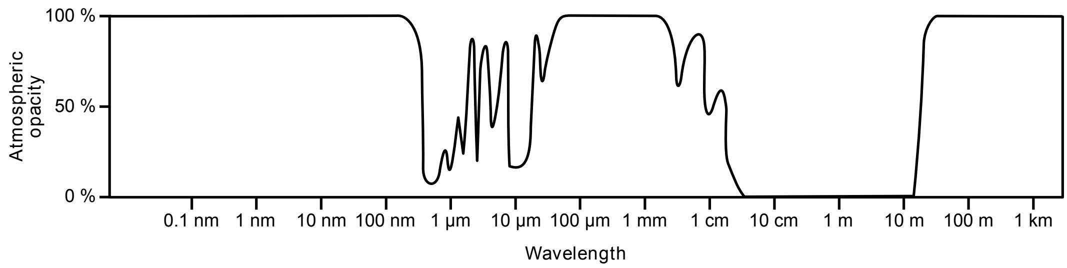

Figure 1.1: Atmospheric electromagnetic opacity for different wavelengths, adapted from [9]

Directive antennas of different types are the most common implementation of radio telescopes. Dish antennas are generally employed for microwave observations [10], while dipole arrays are mostly used for lower frequencies [11]. Anyway, because the resolution of a telescope is proportional to its size (measured in number of wavelengths), single-antenna radio telescopes of feasible sizes are relatively limited in resolution [12].

To overcome this, *interferometry* is used to perform astronomical radio observations with considerably higher resolutions [13]. By combining the measurements of several individual antennas separated by different baselines, an interferometric array can achieve a resolution (though not a sensitivity) equivalent to that of a single telescope with the size of its longest baseline [13].

1.1.2 Low-frequency radio astronomy

Exploration of low-frequency celestial radiation (below 300 MHz) has been mostly carried out using Earth-based interferometric arrays, such as the Very Large Array (VLA) [14], the Giant Metre-wave Radio Telescope [15] and the (more specialized) Low-Frequency Array (LOFAR) [16]. However, as it was mentioned before, these telescopes' observations are limited below 30 MHz because of ionospheric distortions and man-made RFI.

A low-frequency radio telescope deployed in space would intrinsically overcome these limitations [5]. However, the early Radio Astronomy Explorer 2 (RAE-2) satellite [17], launched in 1973, has been the the only realized attempt to explore celestial radiation at frequencies below 30 MHz from space. This mission succesfully covered the band between 25 kHz and 13.1 MHz, but with very limited resolution and sensitivity [18].

Despite the scarce exploration of radio waves with frequencies below 30 MHz, the 30 kHz to 30 MHz band remains as a virtually unexplored spectral window of considerable size (three orders of magnitude), which is very well suited for cosmological and other astronomical studies [5]. The origin of cosmic rays, the dark ages and the epoch of reionization, solar and planetary transients, interstellar plasma and ultra-high energy particles, extra solar planets and even neutrinos could be studied in this band [7, 19].

Because of these relevant scientific drivers, several initiatives to perform space-based ultra-long-wavelength radio astronomy have been developed recently [18]. These initiatives range from several spacecraft containing the different elements of an interferometric array [20] to lunar-based radio telescopes [19].

1.1.3 The OLFAR project

The OLFAR project is one of the initiatives to perform ultra-long-wavelength radio astronomy from space mentioned in Section 1.1.2, which aims to develop a detailed system concept for a large-aperture radio telescope in space to explore celestial radio waves in the very low frequency range of 0.3 MHz to 30 MHz [21].

The radio telescope proposed for OLFAR consists in an *aperture synthesis* interferometric array implemented with a *swarm* of nano-satellites, in which each satellite carries one element of the array [21]. The swarm will be deployed in a suitable orbit that provides the radio quietness required for the scientific observations. Location possibilities include orbits around the Moon, the Earth-Moon L2 point and the Sun-Earth L4/5 point, as well as Earth leading or trailing solar orbits [21].

The satellite swarm concept consists in a system made up of simple (almost disposable) autonomous units, which perform small tasks that contribute to the completion of a common system goal [22]. This way, a swarm shows considerable robustness through redundancy, as well as scalability and self-organization capabilities [23]. However, a satellite swarm also imposes considerable system engineering challenges that must be addressed in order to exploit the advantages of the concept [24].

OLFAR's swarm has three main functions regarding its role as a space-based interferometric array for radio astronomy [25]:

1. observation of celestial radio waves;
2. distributed signal processing of the acquired signals;
3. cooperative downlink to Earth of the processed data.

Figure 1.2 illustrates these functions.

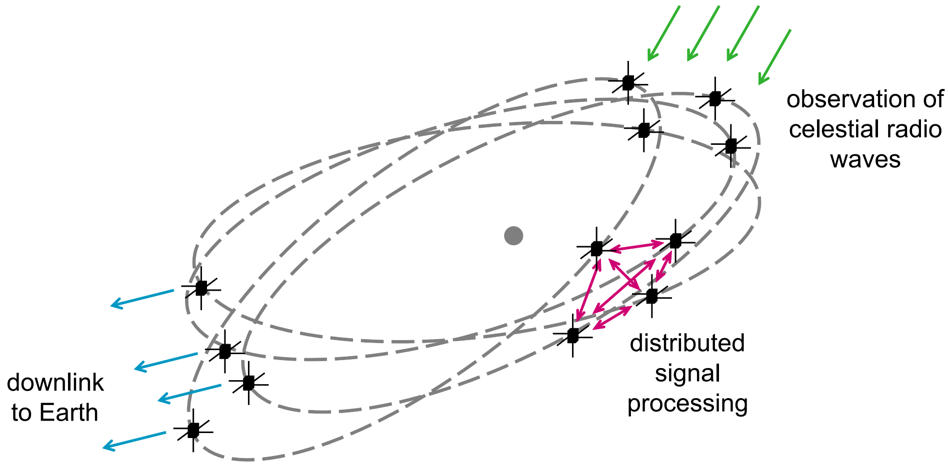

Figure 1.2: Different functions of OLFAR's satellite swarm.

Each element of the swarm should assist in these tasks, which means that each nano-satellite should be able to perform radio observations, share its acquired data with all the other satellites, process a specific frequency sub-band and downlink its processed data to Earth [25]. Figure 1.3 shows the functional components related to these tasks in each nano-satellite, as well as the flow of the involved signals.

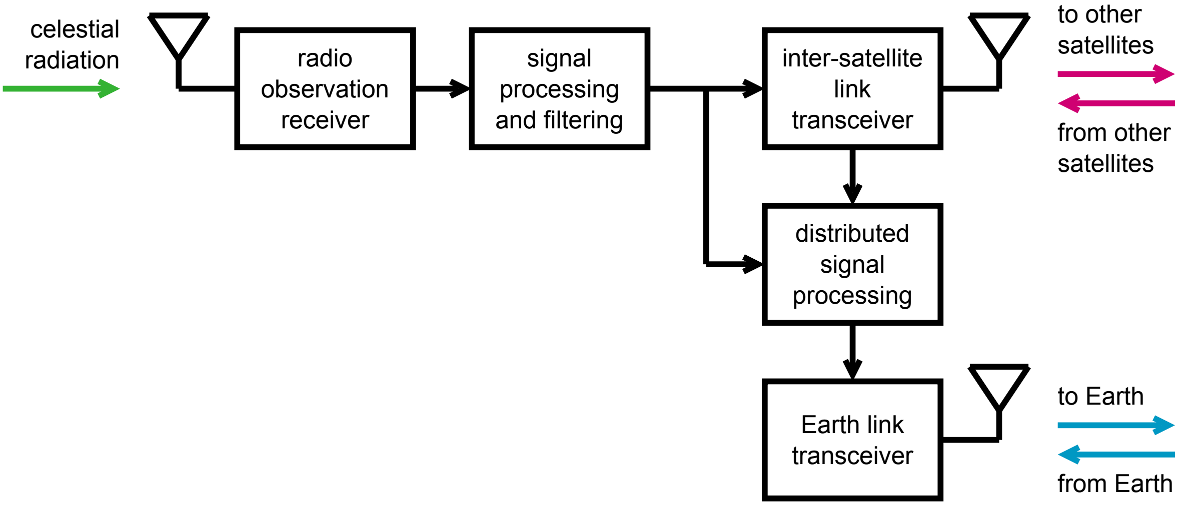

Figure 1.3: Functional components in each nano-satellite.

1.1.4 The inter-satellite link in OLFAR

In OLFAR, the sharing of data among the different satellites will be performed using RF links [25]. This implies unique and challenging requirements for the inter-satellite links (ISL) since the data rate, the element configuration and the satellite properties proposed for OLFAR are considerably different from those present in existing satellite networks with ISLs [26], such as Iridium [27, 28].

OLFAR's inter-satellite communication system consists of three main components (or layers) that provide the essential functions to share information between different nodes through reliable RF links [29]:

1. a data distribution strategy;
2. baseband signal processing;
3. an antenna system.

Figure 1.4 shows how these components make up the ISL block from Figure 1.3.

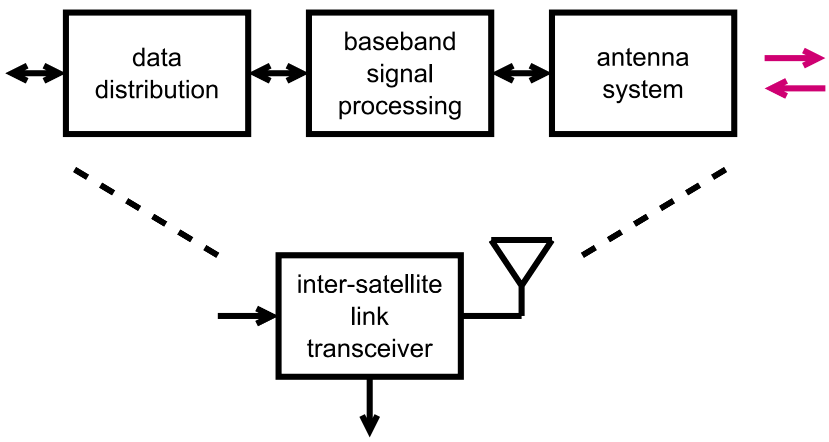

Figure 1.4: Inter-satellite link components in each nano-satellite.

The antenna system for OLFAR's ISL therefore has a critical relevance in the functionality of the swarm and, thus, the project.

1.2 Research goals

The research goal of this work is to develop an antenna system proposal for OLFAR's ISL that can meet the performance required for the astronomical purposes of the project while considering the settings and configurations proposed for its other components. For this, it is necessary to derive clear design requirements and limitations, as well as to identify the aspects of the antenna system that must be addressed in order to achieve an integral solution. Moreover, the performance of the proposal must be evaluated at least analytically and experimentally.

1.3 Report outline

This report presents the results of the design process followed to develop and validate our antenna system proposal. Therefore, in Chapter 2 we analyze the antenna system design problem and indicate the identified requirements and limitations. We describe our proposal in Chapter 3, including the details and motivation of the different design choices. In Chapter 4 we present the validation of our proposal through analytical results obtained using a mathematical model of the ISL. We further validate our proposal with a set of experiments carried out in an evaluation platform. This platform is described in Chapter 5, along with the experiments and the otained results. Finally, conclusions and recommendations for further research make up Chapter 6.

Chapter 2

Problem Analysis

Our design of the antenna system for OLFAR's ISL is influenced by different parts of the concept, which range from the spatial configuration of the swarm to the dimensions of the individual nano-satellites. Based on these, we establish clear requirements and limitations for the antenna system design. In this chapter we present the problem analysis, which involves the scientific observation specifications, the selected ISL communication schemes, the physical properties of the satellites, the radio link characteristics and the link budget.

2.1 Scientific observation

The scientific observation specifications that influence the antenna system design are the amount of information produced by the astronomical measurements and the configuration of the interferometric array.

As shown in Figure 1.3, the radio observation and the initial signal processing in each satellite generate a 'raw' data stream that determines the minimum required throughput of the ISL. In OLFAR, the observation will be performed using direct digital conversion (DDC), while the initial signal processing includes RFI mitigation techniques and filtering, producing a data rate of at most 6 Mbit/s [25].

On the other hand, the spatial configuration of the swarm determines the minimum and maximum distances between satellites, as well as the possible directions for the ISLs. The OLFAR array consists in a constellation of (slowly) free-drifting satellites, with baselines between 10 km and 100 km [25]. This configuration is suitable for OLFAR's scientific purposes, but because of the free drift, the relative location of the satellites with respect to each other changes continuously, even in the presence of attitude control. This means that the ISLs can have—in general—any direction. Figure 2.1 illustrates the variation of the direction of the ISL between two satellites for four time instants.

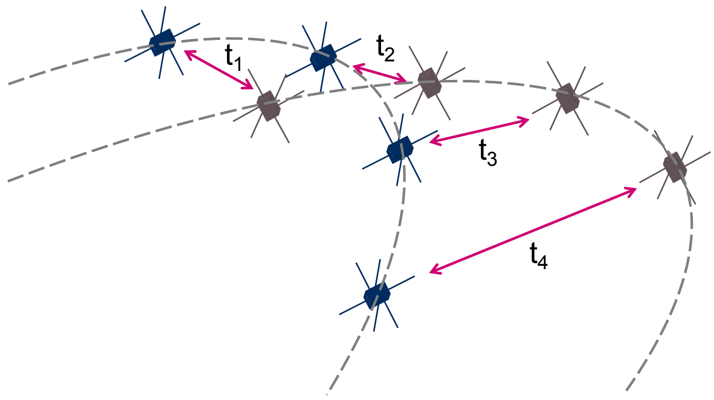

Figure 2.1: Variation of the direction of the inter-satellite link for four time instants (t_1, t_2, t_3 and t_4).

2.2 Inter-satellite communications

The communication schemes selected for OLFAR's ISL have a strong influence in the antenna system requirements, since they basically translate the specifications of the scientific observation (presented in Section 2.1) into a bandwidth and range that the antenna system design must achieve. These schemes, following the structure of Figure 1.4, are the data distribution strategy and the coding, modulation and multiple access techniques.

2.2.1 Data distribution

In OLFAR, an adaptive clustering topology is proposed for the data distribution [30], in which each satellite can take one of two roles:

- observation satellite, or *slave*, which performs the radio observations and shares its data by communicating with its cluster head;
- cluster head, or *master*, which collects the information from the observation satellites belonging to its cluster and distributes it among the other cluster heads.

This scheme provides a reduction in the required resources, namely bandwidth and power, compared to a full-mesh peer-to-peer topology [30].

For OLFAR we consider a maximum of eight slaves per cluster, which imposes a worst-case requirement of 48 Mbit/s over a distance of approximately 90 km for the cluster heads and 6 Mbit/s over 40 km for the observation satellites [29]. Figure 2.2 illustrates the swarm data distribution requirements and their translation on the proposed clustering scheme. Because the cluster heads show the most challenging communication requirements, i.e. longer baselines and higher data rates, we focus our proposal on the cluster-head communications.

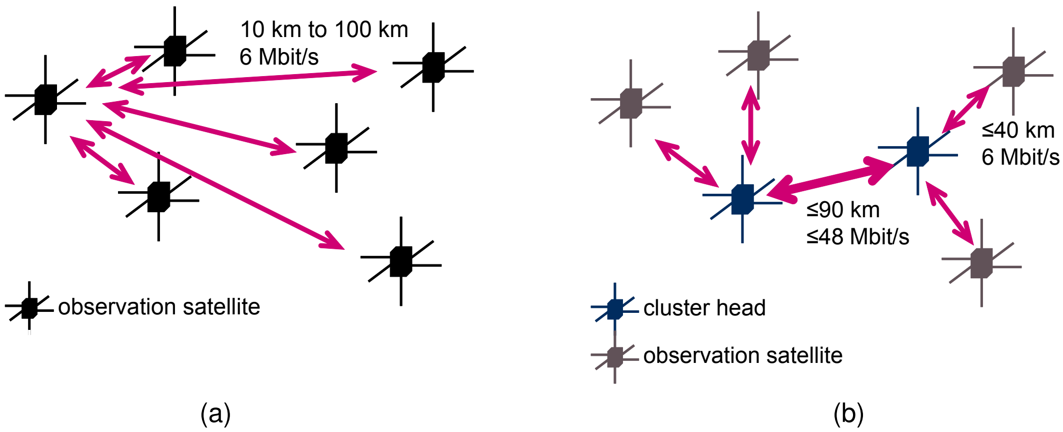

Figure 2.2: (a) Data distribution requirements and (b) their translation on the proposed clustering scheme.

2.2.2 Coding, modulation and multiple access

The coding, modulation and multiple access techniques proposed for OLFAR's inter-satellite communications aim mainly for a sensible balance between spectral and power efficiency. The proposed configuration consists in 3/4 low-density parity-check (LDPC) coding [29], offset quadrature phase shift keying (OQPSK) modulation with raised-cosine pulse shaping [29] and a frequency division multiple access (FDMA) scheme [25]. 3/4 LDPC coding provides considerable coding gain without restrictive latencies, while OQPSK with raised-cosine pulse shaping gives the mentioned balance between bandwidth and power [29].

With this communication scheme, the 48 Mbit/s data-rate requirement for a cluster head imposes a bandwidth requirement of about 32 MHz for the antenna system. Furthermore, a code division multiple access (CDMA) scheme is being studied [29] as an alternative to the initially proposed FDMA approach, since it has proven suitable for high-speed communications between multiple users [31].

2.2.3 Frequency band

The frequency band for OLFAR's ISL has not been fixed yet, but is a fundamental consideration for the antenna system design in terms of antenna size and link performance. As will be discussed in Section 3.4, the antenna implementation proposal changes with the selected frequency band, but it must be anyway above roughly 2 GHz to respect the size limitations (which are presented next). In order to consider a (preliminary) band, we assume that the 2.45 GHz industrial-scientific-medical (ISM) band is used for OLFAR's ISL, since it provides a suitable balance between antenna size, beamwidth and gain (as we will show in Section 3.4).

2.3 Physical properties of the satellites

The dimensions of the nano-satellites proposed for OLFAR and the available power for inter-satellite communications impose significant limitations one the ISLs, since the antenna size and the transmission power have a considerable influence in the capacity of radio links.

Satellites based on a three-unit CubeSat architecture [32], with dimensions of 10 cm $\times$ 10 cm $\times$ 30 cm, are proposed for OLFAR [29]. In such a small device, the inner volume and surface area available for transceivers and antennas dedicated to inter-satellite communications are very limited, considering that it must also carry hardware for scientific observation, distributed signal processing and downlink to Earth, as well as equipment for other systems such as navigation and power management. Figure 2.3 shows the dimensions of a three-unit CubeSat.

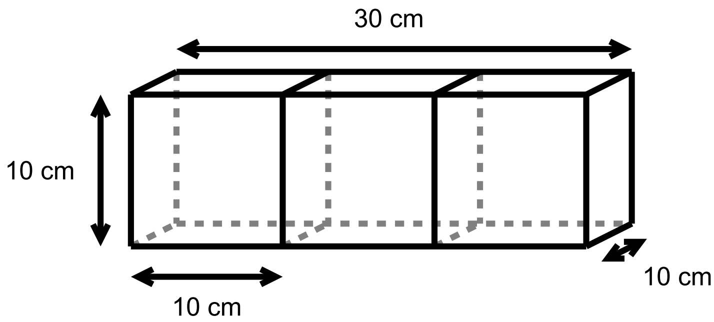

Figure 2.3: Dimensions of a 3-unit CubeSat.

Given this area and volume constraint, the energy harvesting and storaging devices will also be limited in size, and therefore in capacity [22]. Even though a power budget for OLFAR has not been developed yet, an assumption that 4 W are available for transmission of inter-satellite radio signals in a cluster head seems sensible considering that three-unit CubeSats can extract more than 25 W from their solar panels [33].

2.4 Radio link characteristics

For our antenna system design, the relevant radio link characteristics are the channel properties and the validity of the narrowband and far field assumptions. Narrowband, far-field links allow convenient simplifications in their analysis and design, specially for beamforming systems [34].

We consider that the channel for OLFAR's ISL will be roughly free space, so we account only for additive white Gaussian noise (AWGN) and free-space losses, and assume no fading.

For the narrowband assumption, we compare the link bandwidth with the carrier frequency [35]. As it was mentioned in Section 2.2, the radio link between cluster heads has a bandwidth B_{head} of 32 MHz. For a carrier frequency f_{c} of 2.45 GHz, this gives

$$\frac{B_{\text{head}}}{f_{\text{c}}} = 0.013\,, \tag{2.1}$$

which is a good indication that each cluster-head link can be considered narrowband [35]. Nevertheless, the OLFAR swarm involves several cluster heads and many observation satellites, so the overall bandwidth required for inter-satellite communications is much larger. This imposes a restrictive requirement on the bandwidth of the ISL antennas, as will be discussed in Section 3.4.

For the far field assumption, we develop the formal evaluation [31]. For a wavelength λ of 12.24 cm and a largest antenna dimension L_{max} of 3 cm (which we propose in Section 3.4), the Fraunhofer (or Rayleigh) distance D_{F} is [31]

$$D_{\text{F}} = \frac{2\,{L_{\text{max}}}^2}{\lambda} = 1.47\ \text{cm}\,. \tag{2.2}$$

Then, the minimum link distance r_{min} of 10 km is clearly larger than D_{F}, L_{max} and λ, which are the (fully satisfied) requirements for the far field assumption [31].

2.5 Link budget

We analyze the link budget for OLFAR's ISL in order to obtain the required antenna system gain for the considerations mentioned in Sections 2.2 and 2.3, namely the carrier frequency, the link distance and the available transmitter power. In addition to these, we also take into account losses in the transmitter and receiver antenna feeds, the required signal-to-noise ratio (SNR) for $3/4$ LDPC with OQPSK [29] and the receiver noise figure and noise floor derived in Appendix A. Moreover, we consider a minimal link margin of 1 dB, since we are dealing with the worst-case scenario. Table 2.1 shows these parameters and their proposed value. Figure 2.4 shows the link budget structure.

For the proposed link budget parameters and structure, the required overall antenna system gain (i.e. for transmitter and recevier together, $G_{\text{T}} \cdot G_{\text{R}}$) is approximately 10 dB. Since we intend to use the same antennas for transmition and reception, the gain of the antenna system in each satellite (G_{T}, G_{R}) should be at least 5 dB. We show in Section 3.4 that, even though we developed this link budget for 2.45 GHz, an equivalent result holds for other frequencies.

Table 2.1: Link budget parameters.

Parameter		**Proposed value**
Carrier frequency	f_c	2.45 GHz
Link distance	r	90 km
Transmitter power	P_T	36 dBm
Transmitter losses	L_T	1 dB
Friis free-space loss	L_P	139.3 dB
Link margin	LM	1 dB
Receiver losses	L_R	1 dB
Signal-to-noise ratio	SNR	6 dB
Receiver noise figure	NF	4.6 dB
Noise floor	N	-107.1 dBm

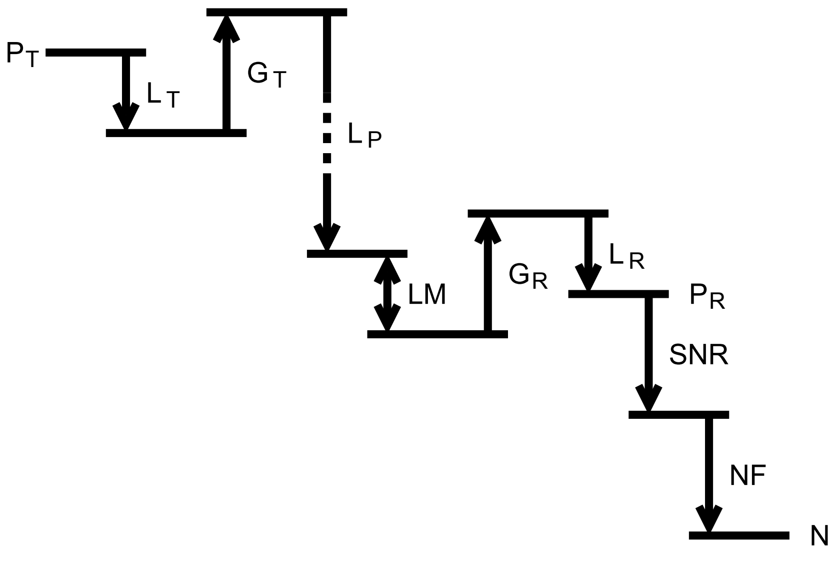

Figure 2.4: Link budget structure.

2.6 Requirements and limitations

From the different considerations, assumptions and results presented before, we identify two requirements and one limitation for the antenna system design. These are shown in Table 2.2.

Table 2.2: Antenna system requirements and limitations.

Requirements	Limitations
The antenna system must provide enough gain for the ISL (at least 5 dBi for 2.45 GHz) The ISL must work for any link direction	The available satellite inner volume and surface area are limited for ISL radio hardware and antennas

These requirements and limitations drive our proposal for the antenna system. In the next chapter we describe this proposal and explain how it satisifies these requisites.

Chapter 3

Antenna System Proposal

In order to meet the requirements presented before, our antenna system proposal should address some specific aspects of the antenna system. In this chapter we describe the approach we take to define which aspects should be considered and develop our antenna system proposal accordingly. For each aspect, the justification of the design choices is discussed, as well as some alternatives that can also provide a feasible implementation.

3.1 Approach

Our proposal consists in an antenna system concept for OLFAR's ISL that can meet the requirements and respect the limitations presented in Table 2.2. In order to be able to cover different directions for the ISL, multiple antennas must be used. Then, an antenna system control scheme is necessary to manage them efficiently. Additionally, the individual antenna characteristics must be studied carefully to ensure that the required gain is available given the area limitations. Finally, the transceiver architecture has an important influence in the flexibility of the system (especially the control scheme), so it should also be considered.

Therefore, with our proposal we address four aspects of the antenna system, which we consider necessary for an integral approach:

- the individual antenna configuration, which consists in the number of antennas and their locations in each nano-satellite;
- the antenna system control, which addresses the strategy used to ensure that the ISL works in any direction;
- the individual antenna characteristics, which comprises their type, size, radiation pattern, polarization, etcetera;
- the transceiver architecture, which discusses the system-level possibilities for the transceiver implementation.

We aimed for a *simple*, *efficient* and *flexible* proposal, looking forward to provide an antenna system solution that can be easily adapted to different requirements and technologies, if necessary.

3.2 Antenna configuration

Since the ISL must work for any link direction, several ISL antennas per satellite are proposed to cover the whole 4π sr (solid angle) range. However, because the satellite surface area is considerably limited, the number of antennas used for the ISL is kept as low as possible.

We propose a configuration of six individual antennas placed on the different faces of each nano-satellite. Considering that the minimum baseline of 10 km is much larger than the satellite dimensions of 10 cm $\times$ 10 cm $\times$ 30 cm, the transmitter in an ISL can be considered as a point source by the receiver. Therefore, the exact location of the antennas in each face is not relevant for the link performance and can be conveniently selected for coexistence with other devices. Figure 3.1 shows the proposed configuration for the antenna system.

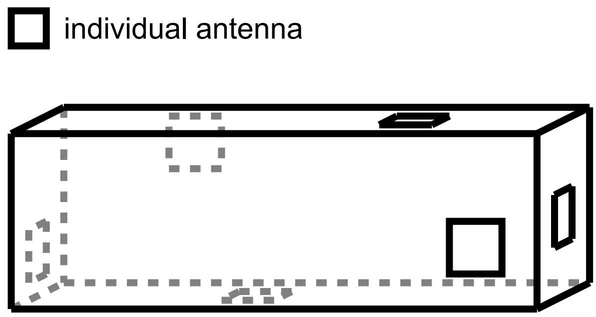

Figure 3.1: Proposed antenna configuration.

With this configuration, each individual antenna must cover a ‘square’ area of $2\pi/3$ sr. However, antenna beams have circular (or elliptical) cross-sections [35]. Then, the required area should be roughly covered by a beam with a circular cross-section and a width of $\pi/2$ (90°). The remaining area that is not covered by the beam can be compensated if the individual antennas have a higher beamwidth, or with an adequate antenna system control (as proposed in Section 3.3). The ‘square’ area coverage required from each individual antenna and its approximation with a circular cross-section beam are shown in Figure 3.2.

For the 2.45 GHz band we must ensure an antenna system gain of at least 5 dBi for any link direction, so each individual antenna must have a gain of at least 5 dBi over the proposed beamwidth of 90°. This requirement for the individual antenna radiation pattern is shown in Figure 3.3.

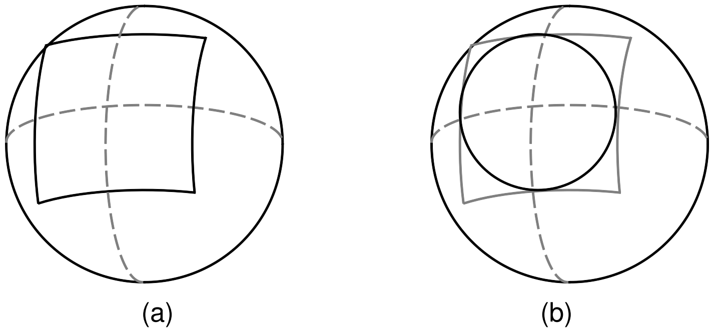

Figure 3.2: (a) 'Square' area coverage required from each individual antenna and (b) its approximation with a circular cross-section beam.

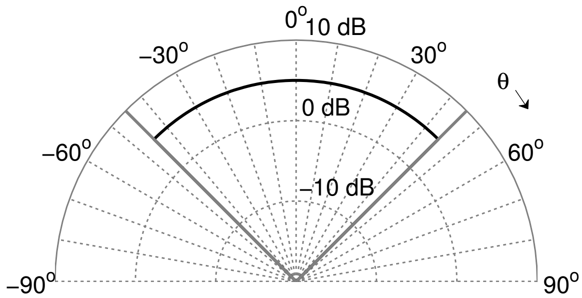

Figure 3.3: Requirement for the individual antenna radiation pattern (for all ϕ).

For an antenna with a circular cross-section beam, the relation between its directivity D and its 3-dB (half-power) beamwidth Θ_{3dB} can be approximated as [35]

$$D \approx \frac{16\,\eta_{\mathrm{b}}}{\left(\Theta_{\mathrm{3dB}}\right)^2}\,, \tag{3.1}$$

where η_{b} is the ratio of power that flows within the 3-dB beamwidth, also known as *beam efficiency* [35]. If the antenna radiation pattern has low side lobes ($\eta_{\mathrm{b}} \geq 0.6$), a directivity of 6 dBi is feasible for a half-power beamwidth of 90° ($\Theta_{\mathrm{3dB}} = \pi/2$).

This last result is independent of the frequency and the antenna effective aperture, and therefore imposes a limitation if higher frequencies are assigned to the ISL, as is discussed in Section 3.4.

If more satellite surface area is available, more antennas with narrower beamwidths and higher gains can be used for the ISL. This would relax the link budget, allowing a higher link margin and/or reducing the power requirements, or could even increase the system capacity.

3.3 Antenna system control

For the antenna system control strategy we propose a *smart antenna* approach [31]. We implement this by multiplying the modulated baseband signal delivered to (or received from) each antenna by a given weight. This weight can be a binary value, which implies a *selection* scheme, or a complex number that conveniently affects the amplitude and phase of the transmitted (or received) signals, allowing for a *combining* scheme. Moreover, depending on the transceiver architecture, ranging and direction-of-arrival (DOA) estimation techniques can be employed in the receiver to determine the location of the transmitter.

For the calculation of the weights we propose a beamforming algorithm that maximizes the antenna system directivity for any link direction $(\theta_\mathrm{d}, \phi_\mathrm{d})$. We assume that for each link direction, at most three individual antennas (X, Y and Z) will participate in the ISL, namely the ones that 'face' the other satellite. Then, we define a coordinate system centered in the corner of the satellite that is common to the faces that hold these antennas. Figure 3.4 shows the definition of the antenna system coordinates for a given set of participating antennas X, Y and Z.

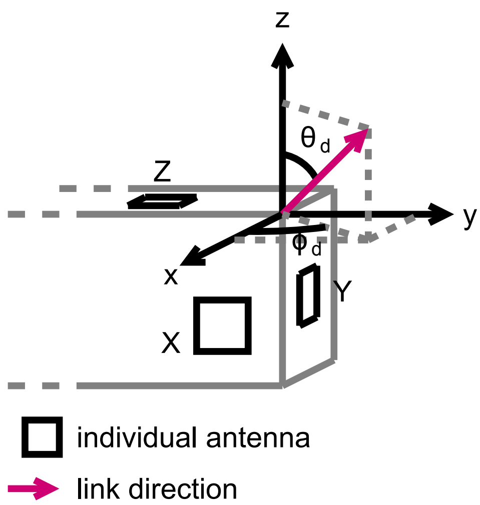

Figure 3.4: Antenna system coordinates.

Furthermore, we assume that for each individual antenna i (where i can be X, Y or Z):

- the link direction refered to its local coordinate system is $(\theta_{\mathrm{d}i}, \phi_{\mathrm{d}i})$, as shown in Figure 3.5;
- the normalized directivity for this link direction is $D_i(\theta_{\mathrm{d}i}, \phi_{\mathrm{d}i})$;
- a sensible approximation of its (power) radiation pattern is known;
- the distance from the antenna system coordinates' origin is d_i.

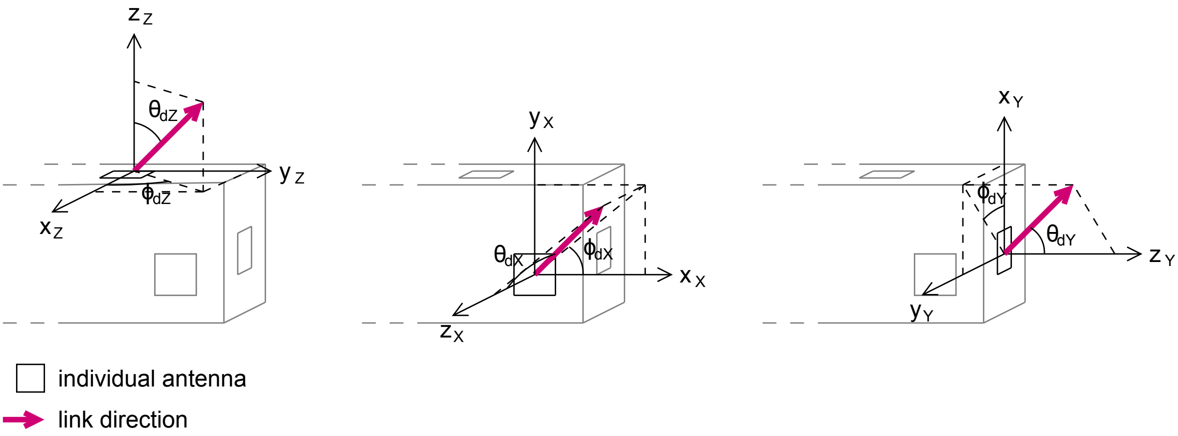

Figure 3.5: Individual antenna coordinates.

Then, the complex weight for each antenna can be calculated as

$$w_i = \sqrt{c_i}\, e^{j\beta_i}\,, \tag{3.2}$$

where

$$c_i = \frac{D_i(\theta_{\mathrm{d}i}, \phi_{\mathrm{d}i})}{\sum\limits_j D_j(\theta_{\mathrm{d}j}, \phi_{\mathrm{d}j})} \tag{3.3}$$

ensures that the power is distributed optimally, and

$$\beta_i = k\, d_i\, \sin\theta_{\mathrm{d}i} \tag{3.4}$$

is the necessary phase change so that, for a wavenumber k, the electric fields (E fields) from the different individual antennas add up in phase.

With this complex weight calculation algorithm, the E fields from the three participating antennas are properly scaled and added up in phase, which gives an increase of up to 4.8 dB (a factor of 3) in the antenna system gain compared to a selection scheme.

Finally, rules for non-linear exceptions can be added to the weight calculation algorithm to increase its precision. For example, an antenna that experiences shadowing by a deployable solar panel for a certain link direction can be suspended from participating in transmission/reception until the link changes to a suitable direction.

3.4 Antenna characteristics

The characteristics of the individual antennas are critical for the performance of the antenna system. Even though in this work a specific antenna design is not proposed, a set of characteristics that they must exhibit are discussed. These characteristics include bandwidth, radiation pattern, polarization, impedance, radiation efficiency and physical area.

3.4.1 Bandwidth

The bandwidth is one of the most restrictive parameters of the individual antennas, and therefore of the antenna system. As we discussed in Section 2.4, the bandwidth for inter-satellite communications in OLFAR includes several cluster-head and observation channels, as well as their corresponding guard bands. Depending on the selected antenna type, it may not be possible to cover the complete ISL bandwidth with one antenna, and a frequency reuse strategy might be necessary. We consider that a minimum bandwidth of 150 MHz provides a sensible balance between antenna feasibility and capacity, specially if microstrip (patch) antennas are used.

3.4.2 Radiation pattern

Different radiation patterns can be used for the individual antennas, as long as they comply with the requirement from Figure 3.3. However, if the proposed beamforming algorithm is used as the antenna system control scheme, a further 3-dB increase can be obtained at $\pm 45^\circ$ in the individual antennas' radiation pattern. Then, an antenna with a gain of 5 dBi and a half-power beamwidth of 90° still provides a (minimal) useful solution.

3.4.3 Polarization

In the same way that in OLFAR's free-drifting constellation the ISLs can take any direction, there can also be any orientation between the transmitting and receiving antennas. Therefore, circular polarization is required for the ISL antennas.

However, since the individual antennas on each satellite have different spatial orientations, an additional phase compensation (with respect to a selected reference antenna) is required in order to perform beamforming for circular polarization. We select antenna Z as the reference because it has the same coordinate orientation as the antenna system. Then, if antenna i radiates an E field in the direction $\mathbf{a}_{\mathrm{E},i}$ for a given link direction, the phase compensation is given by the angle between $\mathbf{a}_{\mathrm{E},i}$ and $\mathbf{a}_{\mathrm{E},Z}$. For a practical implementation, it can be shown that this angle depends on—and can be derived from—the physical orientations of the different individual antennas in each face and the link direction.

3.4.4 Impedance and radiation efficiency

The individual antenna radiation efficiency η_r determines the antenna gain G for a given directivity D [35]:

$$G = \eta_\mathrm{r} \, D \, . \tag{3.5}$$

Then, for an achievable directivity of 6 dBi (as discussed in Section 3.2), the antenna radiation efficiency must be above 80% in order to ensure the required antenna system gain of 5 dBi.

Additionally, the antenna impedance determines its reflection efficiency (for a given feed line) [35]. With appropriate matching (or matching networks) the reflected waves can be minimized, reducing the voltage standing wave ratio (VSWR) [35]. A standard value of 50 Ω is required as the antenna impedance, since most radio equipment (especially amplifiers) use it [31].

3.4.5 Antenna implementation

The antenna implementation, i.e. the type of antenna and its properties, is highly dependent on the frequency band assigned for the ISL and the available satellite surface area, since they strongly influence the antenna dimensions. Given an area restriction, the individual antennas for the antenna system may be implemented using single radiating elements or arrays, depending on the frequency band selected for the ISL.

For the 2.45 GHz band, we propose microstrip (patch) antennas, since they can achieve the previously mentioned characteristics with a very practical form factor. Following a simplified design procedure for patch antennas [35], the required length L and width W of a ceramic patch antenna with a relative dielectric constant ε_{r} of 5.4 and a resonance frequency f_{c} of 2.45 GHz are, respectively, 2.6 cm and 3.4 cm. This means that each individual patch antenna would fit in an area of roughly 9 cm^2. For a three-unit CubeSat, in which the smallest face has dimensions of 10 cm $\times$ 10 cm, we consider that this area could be available on each satellite face for ISL antennas, although it might be close to the maximum.

Despite of their convenient form factor, patch antennas are—in general—limited in bandwidth [35]. Although it is possible to build wideband patches with the proposed beamwidth and gain [36], a careful design of the antennas used for the ISL must be performed. As an alternative, helical antennas show better bandwidth and impedance characteristics, but have considerably larger dimensions than patch antennas (although they might require the same area).

For higher frequencies, the available area must be exploited as much as possible so that the link budget from Section 2.5 remains valid. The 5 dBi gain requirement obtained for 2.45 GHz actually implies a necessary effective area [31]

$$A_{\text{eff}} = \frac{\lambda^2}{4\pi} G_{\mathrm{R}} = 37.67\ \mathrm{cm}^2\,, \tag{3.6}$$

which is independent of frequency. Therefore, this is the requirement that antennas must fulfill for any frequency band. If the frequency increases, higher gain is required to achieve the same effective area. From 3.1, the beam efficiency must be higher to obtain a higher gain (given the required beamwidth of 90°), which means more demanding requirements on the antenna radiation pattern.

If the frequency is high enough, it may not be possible to obtain the required effective area and beamwidth with a single element. Then, the use of several antennas in planar phased arrays is proposed, at the expense of increased complexity and radio hardware. An array would have a narrower beamwidth and higher gain, but would also be able to steer its beam over the $\pm 45^\circ$ range. For an array of N_elem elements, the required element gain G_elem over the proposed 90° range is

$$G_\mathrm{elem} = \frac{1}{N_\mathrm{elem}} \frac{4\pi}{\lambda^2} A_\mathrm{eff} , \tag{3.7}$$

which could become a feasible requirement. Figure 3.6 illustrates the implementation possibilities with a single patch antenna and a planar array.

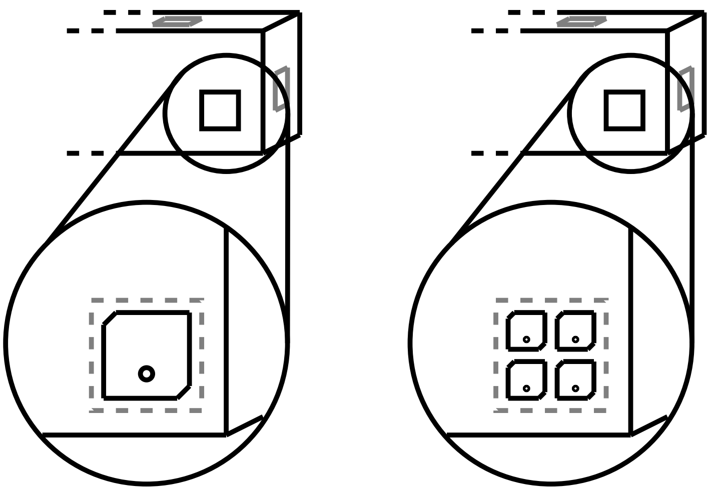

(a) (b)

Figure 3.6: Individual antenna implementation with (a) a single patch antenna and (b) a planar array.

3.5 Transceiver architecture

The performance of the different possible control schemes is significantly influenced by the ISL transceiver architecture. The weight multiplication proposed for the smart antenna control scheme can be implemented as an analog RF or a digital baseband block [31], as shown in Figure 3.7. For example, a selection scheme can be efficiently implemented with analog RF control, which in this case would be performed using switches. For a combining scheme like the proposed beamforming algorithm, analog RF control would consist in phase shifters and variable gain amplifiers, while digital baseband control would use an application specific integrated circuit (ASIC) or a field programmable gate array (FPGA).

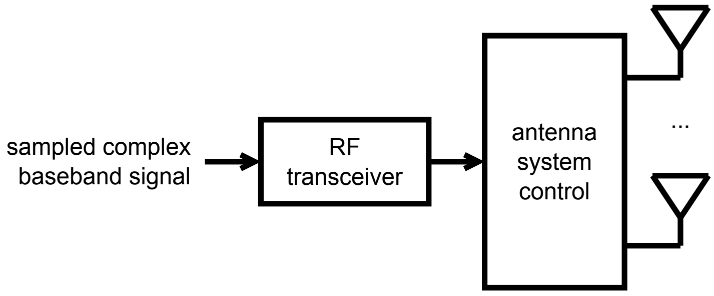

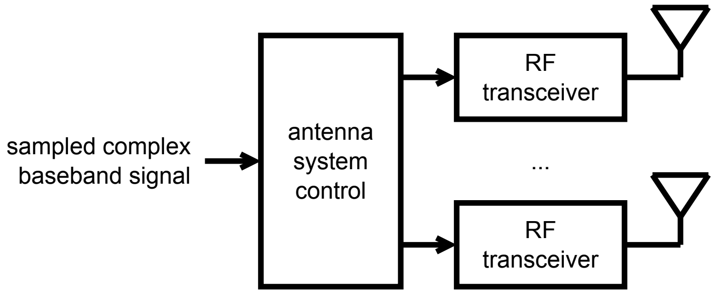

Figure 3.7: Transceiver architecture with (a) analog RF and (b) digital baseband control.

While analog RF control is less flexible (and in general less precise), it requires considerably fewer components since only one RF transceiver is necessary. On the other hand, digital baseband control is far more flexible and precise, but requires more radio hardware. We assume that the RF transceiver integration can be such that the additional hardware does not impose a significant volume load, and that the power requirements of the extra transceivers fall within the power budget. Thus, we propose digital baseband control for OLFAR's ISL transceiver.

Irrespective of the selected transceiver architecture, the antenna system control block consists in a controller that performs the weight calculation and an implementation of the weight multiplication. Figure 3.8 shows the structure of the antenna system control block for digital baseband control. For this implementation, the controller takes the sampled complex baseband signals from each antenna, estimates their received power and phase, performs DOA and range estimation to determine the location of the transmitter and calculates the weights that correspond to the identified link direction. This process should be repeated at a rate that is proportional to the relative speed between the transmitter and the receiver. Figure 3.9 shows the functional components of the proposed antenna system controller.

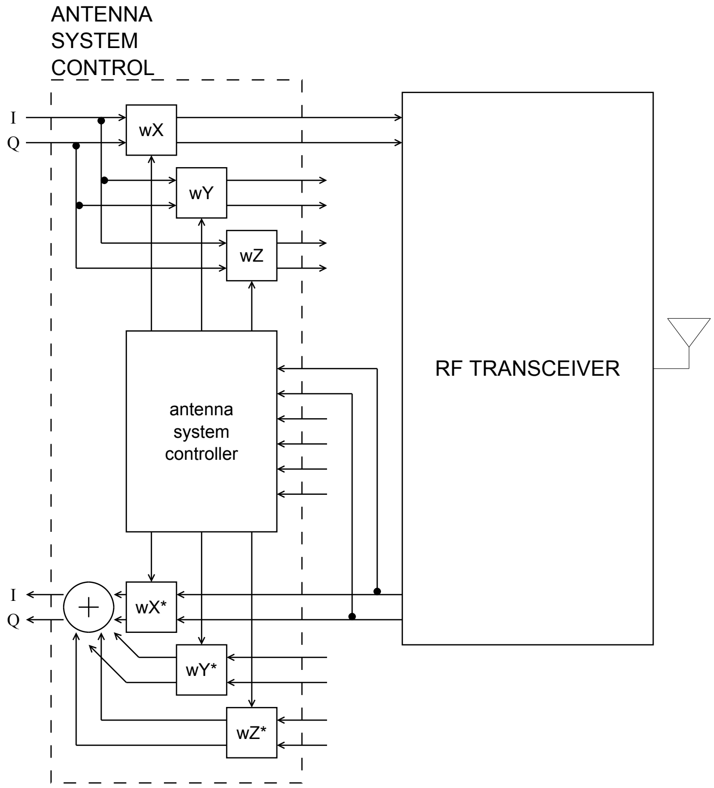

Figure 3.8: Antenna system control structure.

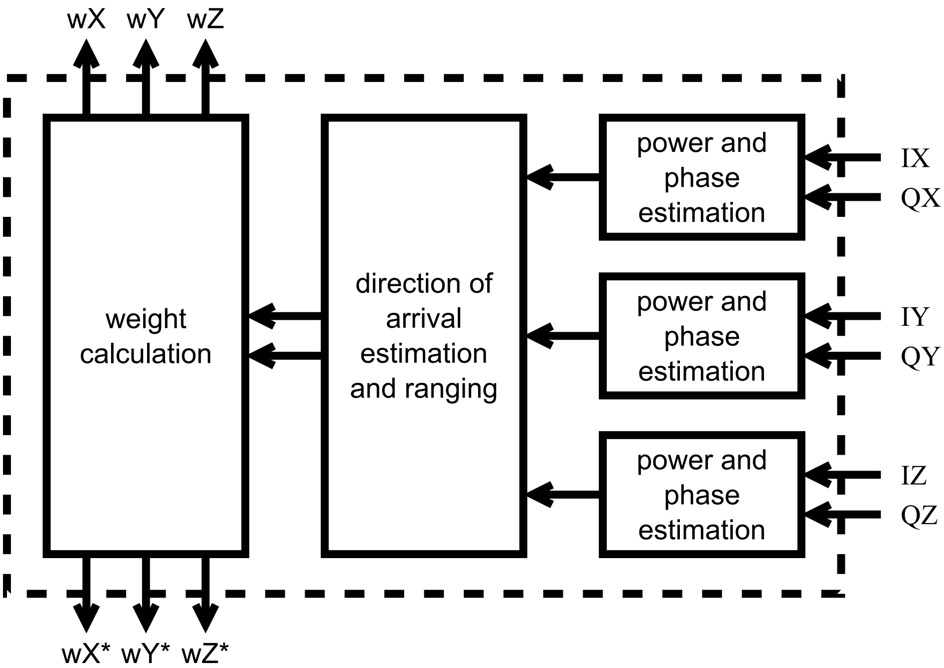

Figure 3.9: Antenna system controller functional components.

The proposed antenna configuration, control scheme, individual antenna characteristics and transceiver architecture were devised to comply with the requirements and limitations presented in Table 2.2. However, in order to validate our design we developed an analytical model and an experimental platform, in which the performance of the proposed antenna system was evaluated. The following chapters (4 and 5) present, respectively, the developed analytical model and experimental platform, as well as the results obtained from them.

Chapter 4

Analytical Results

In order to evaluate our proposal for OLFAR's ISL antenna system, we implemented an analytical model of the link, which includes the individual antenna radiation pattern, the antenna configuration and the proposed beamforming algorithm. In this chapter we describe the developed analytical model and present the results obtained from it.

4.1 Analytical model

The analytical model for the ISL was developed in Matlab, and it calculates the antenna system's radiation pattern for any link direction. This way, the performance (in terms of gain) of the proposed beamforming algorithm can be evaluated for any direction of the ISL. The model consists of five functional parts:

- an individual antenna radiation pattern model, used to simulate the gain and E field of each individual antenna for a given link direction;
- a 3D satellite model, used to represent the individual antenna locations and orientation;
- an antenna system controller, used to implement the weight calculation algorithm;
- a field/signal calculator, used to obtain the resulting transmitted field and the combined received signal of the antenna system;
- a channel simulator, used to model the effects of the channel.

These parts are organized in the structure shown in Figure 4.1.

With this architecture, the individual antenna model, the antenna configuration and the control scheme can be changed independently of each other, making the ISL model flexible enough to evaluate the antenna system performance considering different combinations of characteristics.

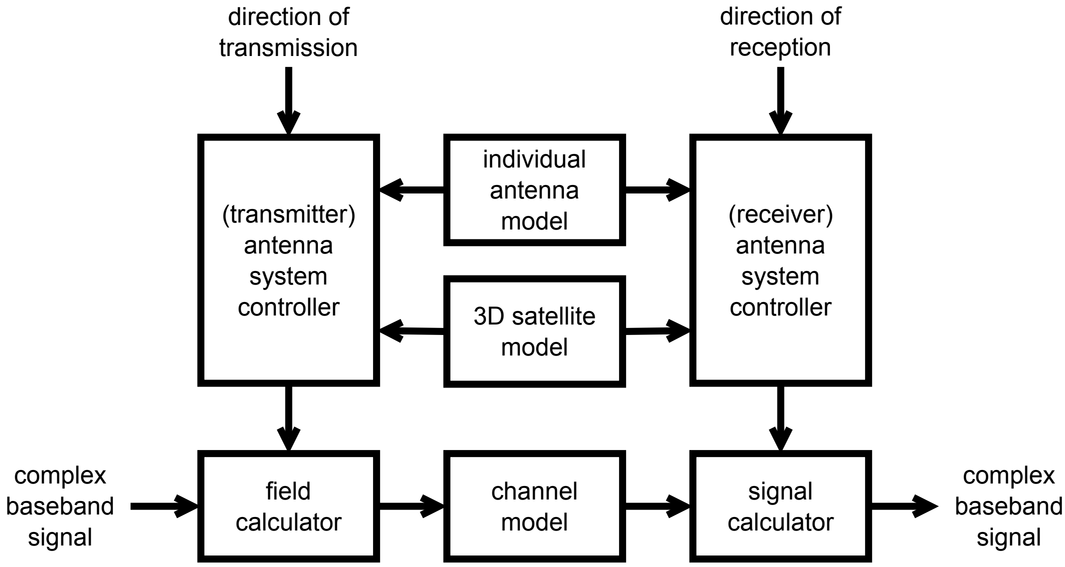

Figure 4.1: Structure of the analytical model.

The model uses far-field and narrowband approximations, and neglects coupling since the interaction between E fields of different antennas is relatively low. Three-dimensional complex-valued vectors are used to represent the E fields, which simplifies the simulation of circular polarization. The global and individual antenna coordinate systems presented in Figure 3.4 and Figure 3.5 are also considered in the model, in order to be consistent with the presented proposal.

Finally, since noise and propagation loss hardly affect the performance of the beamforming algorithm under the mentioned assumptions, the implemented channel model includes only the orientation difference between the transmitting and the receiving satellites, implemented using Euler rotations [37].

4.2 Simulation settings

4.2.1 Individual antennas

A basic individual antenna radiation pattern with 5 dBi gain and 90° half-power beamwidth, described by $\cos^2(\theta)$ and shown in Figure 4.2 was used. This radiation pattern provides the minimum gain and bandwidth requirements for the individual antennas, as mentioned in Section 3.3.

As mentioned before, the use of complex-valued vectors for the E fields allows the simulation of circular polarization. Figure 4.3 shows the field directions for one of the modelled circularly polarized antennas.

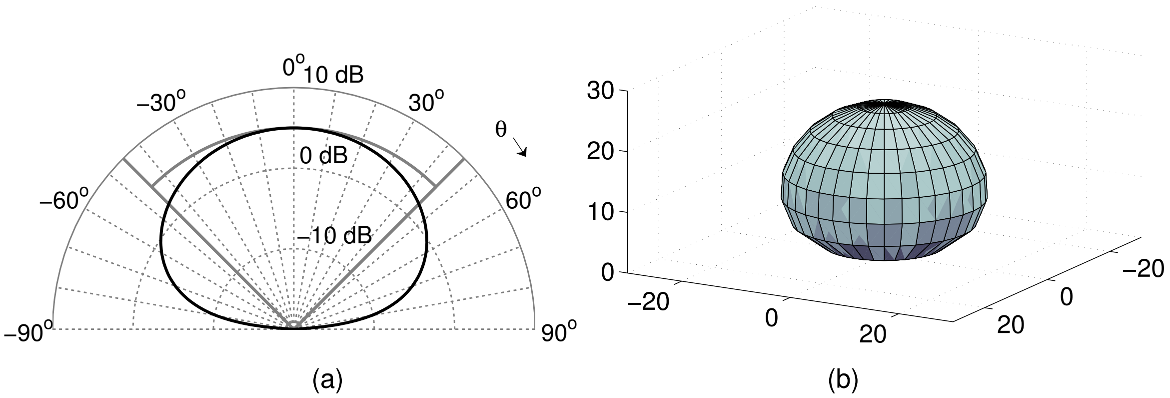

Figure 4.2: Modelled individual antenna radiation pattern in (a) 2D (for all ϕ) and (b) 3D.

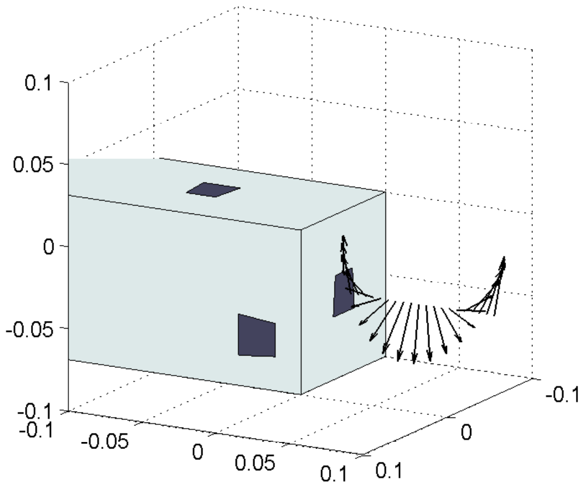

Figure 4.3: Modelled individual antenna circular polarization.

4.2.2 Satelite model

A three-unit cubesat model with antennas on three faces (corresponding to X, Y and Z) placed in arbitrary positions was used. Figure 4.4 shows the satellite model, in which the orientation of each individual antenna can be appreciated. This orientation, along with the link direction, is used to determine the required phase compensation for circular polarization mentioned in Section 3.4.

4.2.3 Channel model

As mentioned before, the channel model includes only the orientation difference between the transmitter and the receiver. Figure 4.5 shows the orientation of the receiver satellite model, rotated arbitrary angles in a 3-2-1 sequence.

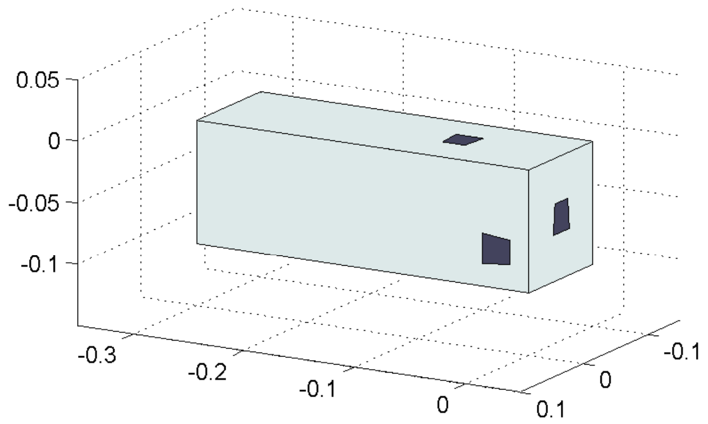

Figure 4.4: Satellite model.

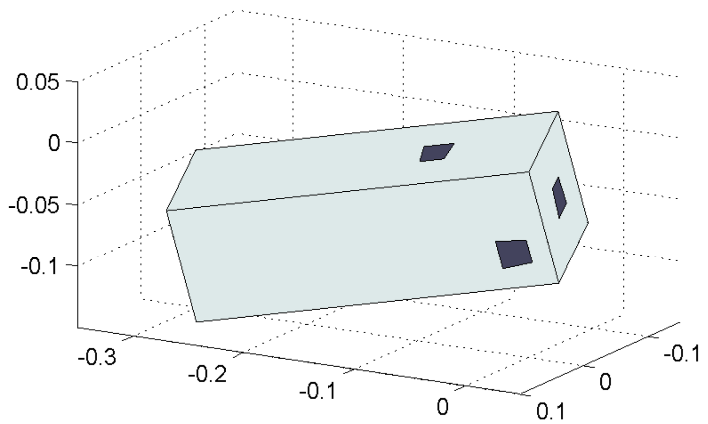

Figure 4.5: Orientation of the receiver satellite model.

4.3 Results

The resulting antenna system radiation patterns for an arbitrarily selected link direction $(\theta_{\mathrm{d}}, \phi_{\mathrm{d}})$ of $(58.1°, 38.3°)$ using the proposed beamforming algorithm and an antenna selection scheme are shown in Figure 4.6 and Figure 4.7. The antenna system controller shows the expected performance, since the proposed beamforming algorithm gives an antenna system gain of 5 dBi, about 3 dB over the gain given by the selection scheme.

Additionally, the gain of the proposed antenna system was obtained for different link directions, to show that the beamforming algorithm ensures maximal antenna system gain for all link directions, even using individual antennas with the minimun gain and beamwidth requirements. The obtained results are shown in Figure 4.8, along with the results for a selection scheme. Because the control schemes work symmetrically for $\phi_{\mathrm{d}} = 0°$, $\phi_{\mathrm{d}} = 90°$ and $\theta_{\mathrm{d}} = 90°$, Figure 4.8 shows only one of these cases.

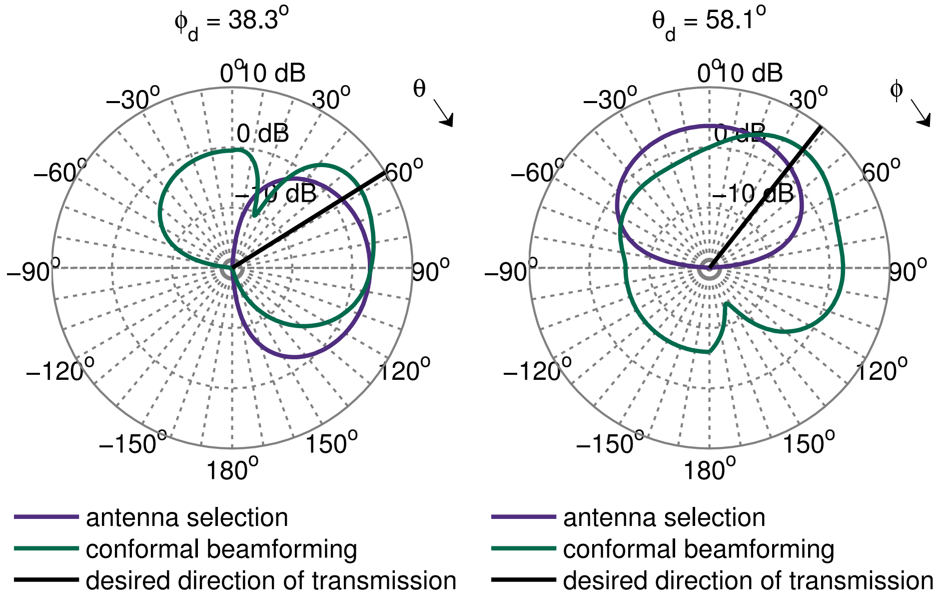

Figure 4.6: Antenna system radiation pattern for $(\theta_\mathrm{d}, \phi_\mathrm{d}) = (58.1°, 38.3°)$.

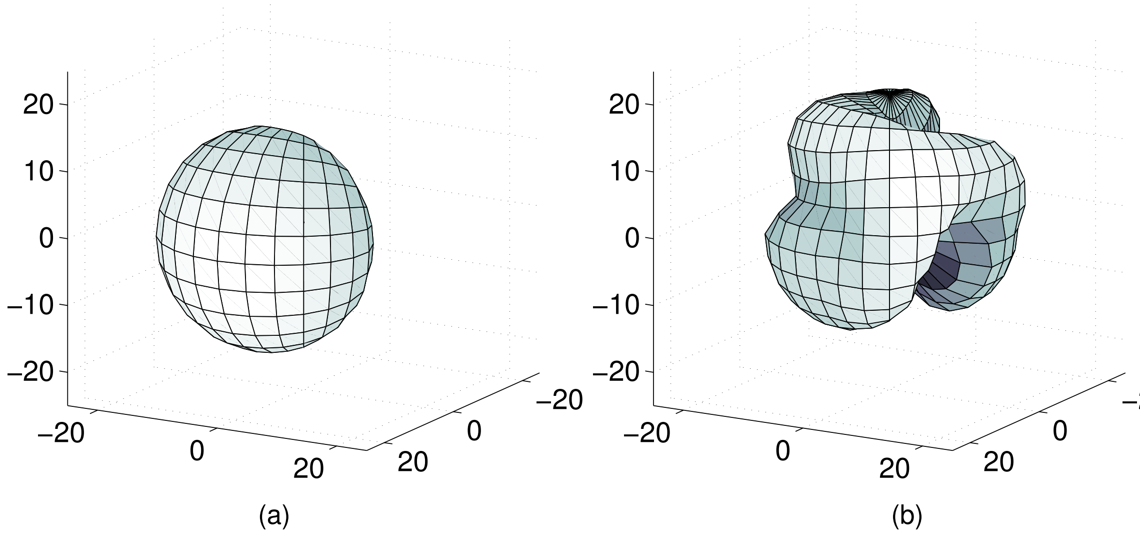

Figure 4.7: Antenna system 3D radiation pattern for $(\theta_\mathrm{d}, \phi_\mathrm{d}) = (58.1°, 38.3°)$ using (a) a selection scheme and (b) the proposed beamforming algorithm.

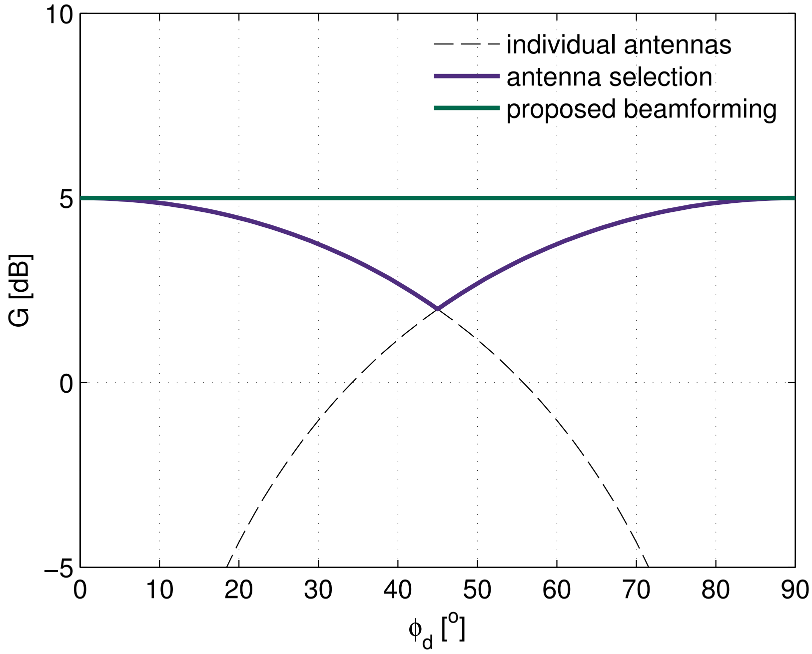

Figure 4.8: Antenna system gain for different link directions (for $\theta_\mathrm{d} = 90°$) obtained with the analytical model.

4.4 Conclusion

The results obtained from our analytical model show that the proposed antenna system with the beamforming algorithm can ensure, theoretically, a system gain of 5 dBi for any link direction, even with the minimal useful individual antenna radiation pattern. This shows that the proposed requirements for the antenna system can be met with the beamforming scheme in a scenario in which a simple antenna selection would not provide the required performance.

Chapter 5

Experimental Results

To further validate our antenna system proposal for OLFAR's ISL, an experimental evaluation platform was developed to emulate the antenna configuration and to implement a control scheme. An experiment was then carried out on the platform to evaluate the performance of the proposed beamforming algorithm. In this chapter we describe the developed platform and present the results obtained from it.

5.1 Evaluation platform

The evaluation platform was designed and implemented mainly to test the proposed beamforming algorithm. However, it also worked as an exercise to explore currently available technologies that are suitable for the implementation of the antenna system. Moreover, with some improvements it can be used for further experimentation and testing of other parts of the ISL.

The platform consists in one ISL transmitter and one ISL receiver, representing a uni-directional link between two satellites. Two complete channels were implemented in both the transmitter and receiver, in order to use baseband digital control between two antennas on each side. This way, a two-dimensional (2D) simplification of the beamforming algorithm could be evaluated.

5.1.1 Transmitter and receiver structure

The transmitter developed for the evaluation platform consists in a baseband digital processor, two digital-to-analog converters (DACs), two analog in-phase/quadrature (IQ) modulators and two patch antennas. The receiver is made up of two patch antennas, two low-noise amplifiers (LNAs), two analog IQ demodulators, two analog-to-digital converters (ADCs) and a baseband digital processor.

Because a baseband signal with low bandwidth is enough to test the proposed control schemes, high-speed baseband digital components were not used in the evaluation platform, although they might be added in the future. Therefore, personal computers (PCs) running Matlab were used as the baseband digital processors, with dedicated digital interfaces to interact with the DACs or ADCs. For these digital interfaces, a universal serial bus (USB) connection is suitable for communication with the PC and a serial peripheral interface (SPI) is fast enough to communicate with the DACs and ADCs. Finally, the analog connection between the DACs/ADCs and the IQ modulators/demodulators is performed with differential interfaces.

Figure 5.1 shows the evaluation platform architecture. The specific components used to implement each block are shown in Figure 5.2, and their most relevant specifications are presented in Table 5.1.

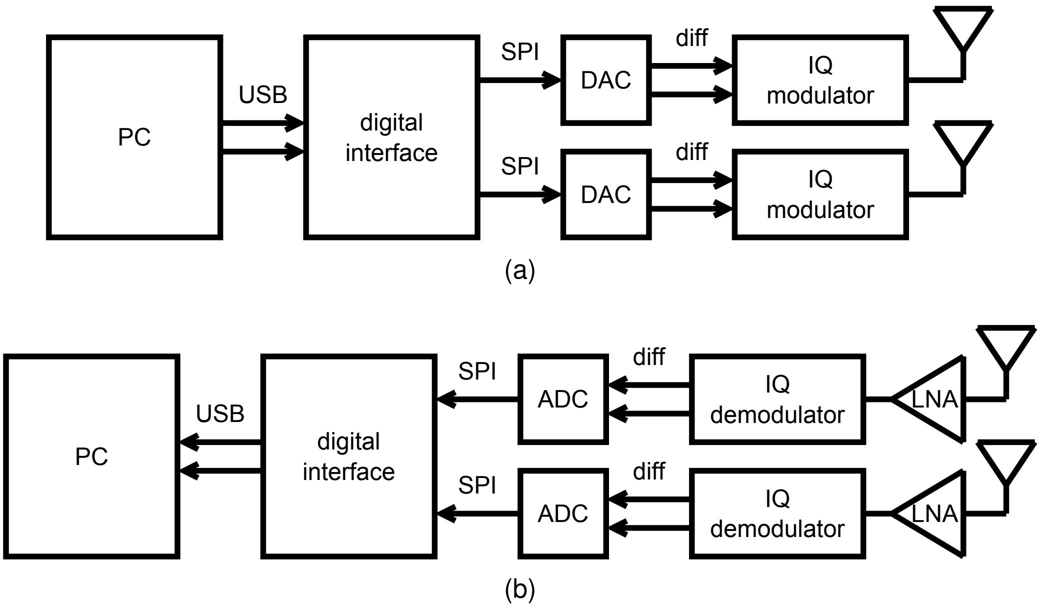

Figure 5.1: Evaluation platform (a) transmitter and (b) receiver architecture.

The transmitter and receiver use a common carrier signal for both of their channels, in order to provide the oscillator synchronization required for beamforming [34]. Nevertheless, compensation for phase differences in the carrier signals of the two channels can be performed through the baseband complex weights, as long as these differences are known.

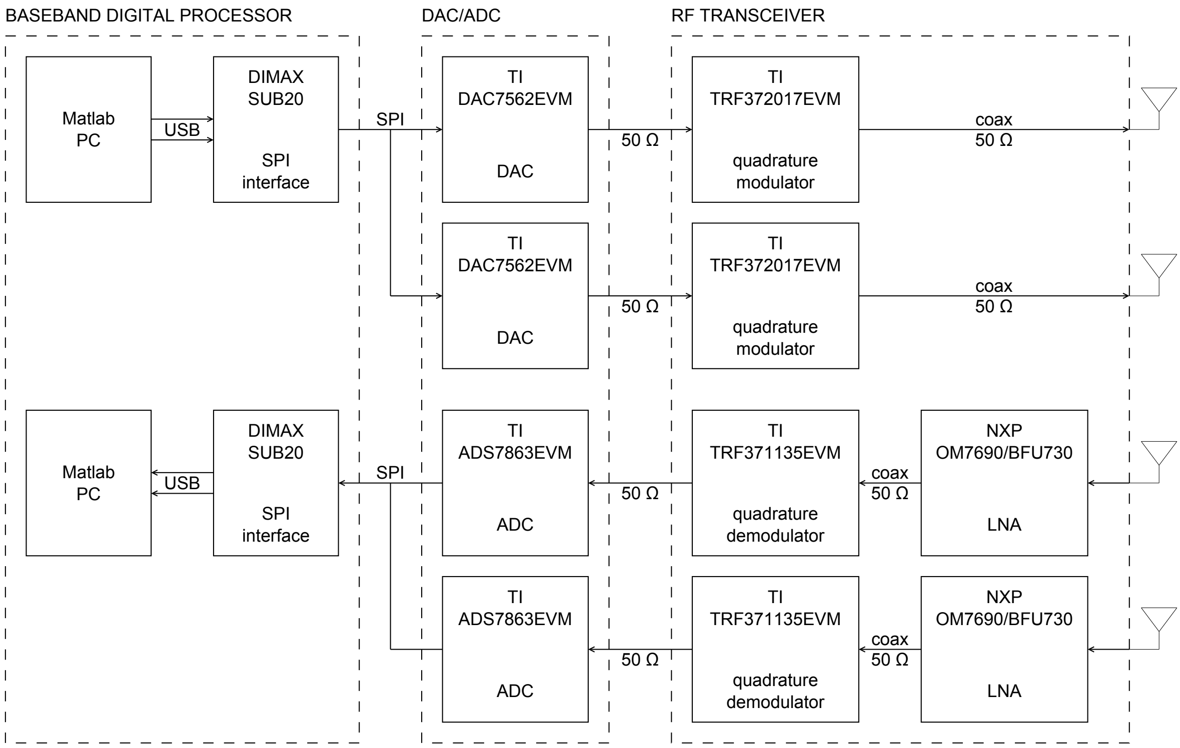

Figure 5.2: Specific components used for the evaluation platform.

Table 5.1: Evaluation platform component specifications.

Component	Relevant specifications
Digital interface	8 MHz SPI
Digital-to-analog converter	10 μs settling time 12 bits 2 channels
Analog-to-digital converter	2 MS/s 12 bits 2 channels
Integrated IQ modulator	300 MHz – 4.8 GHz integrated LO -2.7 dB voltage gain
Integrated IQ demodulator	2.3 GHz – 2.7 GHz balun 43 dB gain 13 dB noise figure
Low-noise amplifier	2.3 GHz – 2.7 GHz 21 dB gain 0.8 dB noise figure
Patch antenna	2482 MHz center frequency 85 MHz bandwidth right-hand circular polarization 5 dBi gain 50 Ω impedance 0.83 efficiency

5.1.2 Antenna configuration

The platform configuration includes two satellite 'simulators', separated by 80 cm, each with two aluminium 'faces' of 10 cm $\times$ 10 cm that act as ground planes for the patch antennas that are placed on their center. This works as a representation of antennas X and Y from Figure 3.4. The satellite 'simulators' can be rotated over their own axes to simulate a difference in orientation between the transmitter and the receiver, which in this case corresponds to a variation in ϕ_{d}. Figure 5.3 shows the dimensions and configuration of the evaluation platform.

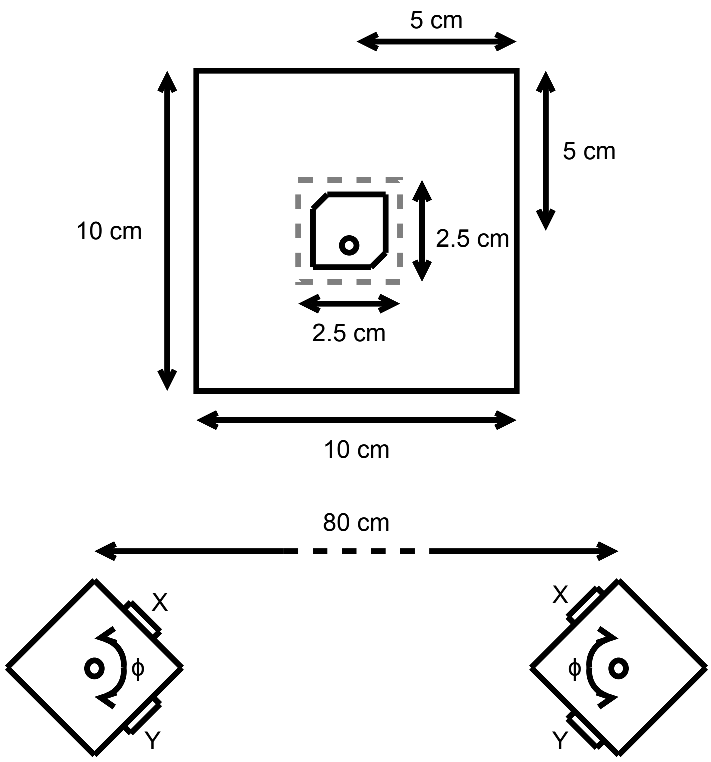

Figure 5.3: Evaluation platform dimensions and configuration.

The individual antennas used in the evaluation platform have a specified radiation pattern that is very similar to the one assumed for the analytical model, including a gain of 5 dBi and a 3-dB beamwidth of approximately 90°. Therefore, the individual antenna model from Figure 4.2 can be used as an estimation of the real antenna radiation pattern required for the control scheme. Figure 5.4 shows the radiation pattern of the antennas used for the evaluation platform, along with its relevant specifications.

Despite of this radiation pattern specification, the real pattern exhibited by the antennas placed on the satellite simulators might change slightly, depending on the properties of the ground plane (i.e. its size and electrical properties [38]) and the coupling between antennas in different faces of the satellite [31].

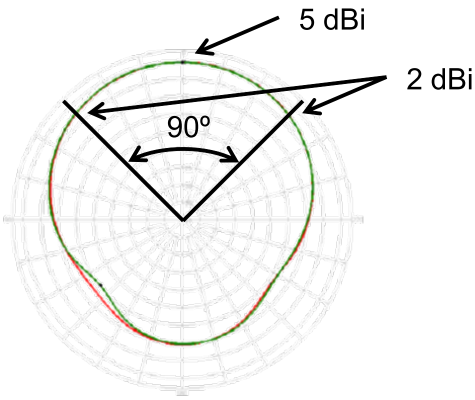

Figure 5.4: Radiation pattern of the antennas used in the evaluation platform, adapted from [38].

5.2 Experiment settings

To evaluate the performance of the antenna system controller, only the analog components of the platform were used (i.e. the antennas, LNAs and IQ modulators and demodulators). This is because the integrated IQ modulators require a minimum baseband input bandwidth (not specified in their datasheets) that the Matlab-running PC could not achieve.

The baseband input signal used for the experiments was a sinusoid of 1 V peak-to-peak amplitude at 50 kHz, which was applied to both the in-phase (I) and quadrature (Q) inputs of one transmitter. The evaluation of the control scheme was performed in the receiver, post-processing the measured IQ signals obtained from each antenna (X and Y). However, instead of the 'blind' beamforming weighting from the proposed algorithm, a maximal ratio combining (MRC) [31] diversity technique was employed, since it converges to the beamforming behavior in the analytical model but shows a considerable performance increase in practical situations.

The experiments were performed in an anechoic room provided by the Netherlads Institute of Radio Astronomy (ASTRON), located in Dwingeloo. Figure 5.5 shows the implemented setup in the anechoic room.

5.3 Results

The same evaluation of the antenna system gain for different link directions carried out with the analytical model (and shown in Figure 4.8) was performed in the evaluation platform. The received signal power was measured for different values of ϕ_d (from 0° to 90° in steps of 7.5°), and the normalized antenna system gain was calculated. These results are shown in Figure 5.6.

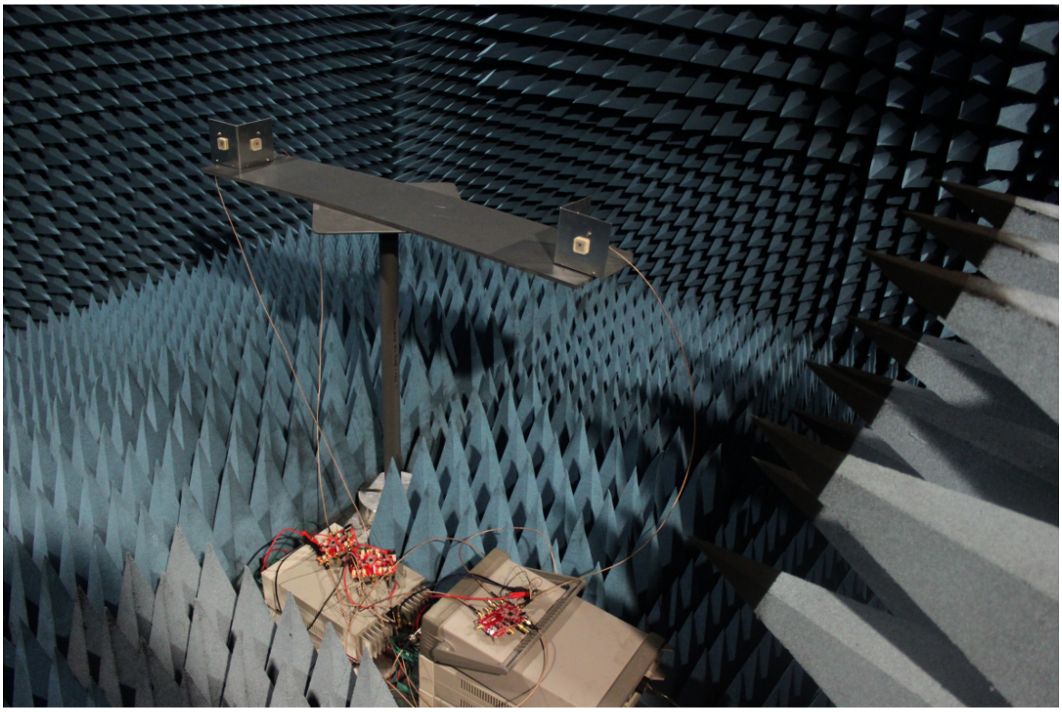

Figure 5.5: Evaluation platform in the anechoic room.

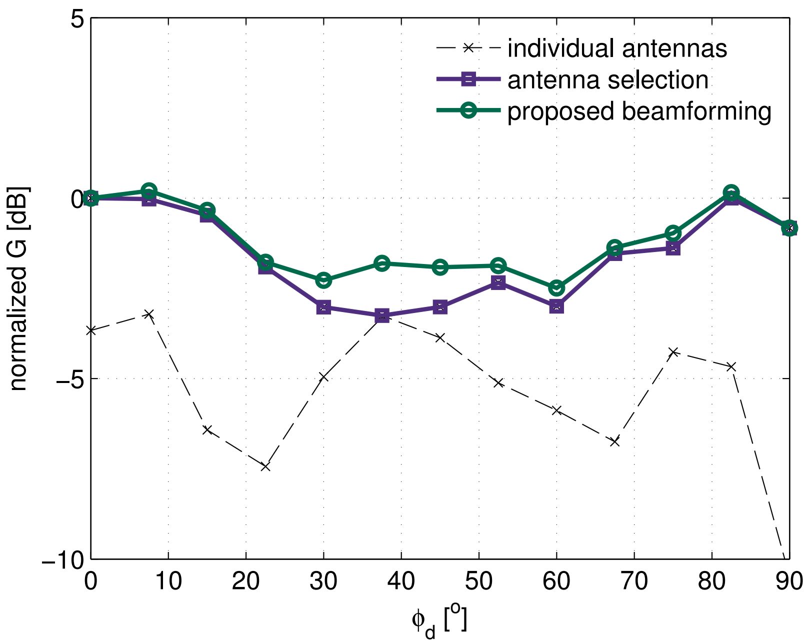

Figure 5.6: Antenna system gain for different link directions (for $\theta_{\mathrm{d}} = 90°$) obtained with the evaluation platform.

In the experimental evaluation, the antenna system did not achieve the ideal performance of the analytical model, but the implemented MRC scheme managed to still provide a gain improvement of about 2 dB over the antenna selection scheme for link directions around 45°. This means that the control scheme in the receiver can provide a gain improvement close to the theroetical 3 dB presented in Figure 4.8, but the individual antennas didn't show the specified radiation pattern from Figure 5.4.

The difference between the specified and obtained individual antenna radiation patterns, as discussed in Section 5.1, is mainly due to the coupling between the fields from the two antennas and the characteristics of the ground plane. On the other hand, the 1-dB reduction in the performance of the control scheme could have been caused by a multipath component introduced by the polyvinyl chloride (PVC) board used to support (and align) the transmitter and receiver.

5.4 Conclusion

Despite of the differences observed between the analytical and experimental evaluation of the antenna system proposal (especially Figures 4.8 and 5.6), we consider that the obtained experimental results are sufficient to demonstrate that the MRC control scheme shows a satisfactory performance, since it provided a system gain improvement close to the one obtained from the analytical model. Moreover, we also conclude that the evaluation platform can give valuable insight on the performance of the proposed antenna system regarding other aspects, like the individual antenna radiation pattern.

We consider that the experimental performance of the antenna system can be improved if the coupling between the fields of the individual antennas is modelled and compensated and an alternative (mechanical) structure is used for the transmitter and receiver.

Chapter 6

Conclusions and Recommendations

Based on the presented problem analysis, design approach, solution proposal and obtained anaytical and experimental results, in this chapter we present some conclusions and recommendations for future work.

6.1 Conclusions

We have presented an antenna system proposal for OLFAR's ISL that addressed the antenna configuration, the control scheme, the antenna characteristics and the transceiver architecture. We derived this proposal from a comprehensive problem analysis that led to the definition of a set of requirements and limitations for the antenna system. Moreover, we have also presented analytical and experimetal results that support the proposal, which are based on an analytical model and an evaluation platform developed for the project.

The proposed antenna system concept aims to carefully respect the defined requirements and limitations, and therefore consists in a conservative configuration (in terms of surface area) of six antennas and its required antenna characteristics, along with a tailored beamforming control scheme and its corresponding ideal transceiver architecture. This provides an efficient solution that fulfills the design objectives (although further experimental tests are required), and that shows significant flexibility in the sense that its different parts are relatively modular and can be modified for different conditions and requirements.

However, this efficiency and flexibility come with a significantly high system complexity. Independent transceivers are required for each antenna, and the proposed combining scheme requires significant processing power and speed. Moreover, the ambitious requirements and limitations set for the antenna system restrict the implementation alternatives, which leaves little room for simplification. For example, if we relax the surface area limitation, the possibility of using more than six antennas (in more than six perpendicular directions) with higher gains and narrower beamwidths would relax the link budget and allow the use of a selection control scheme, which requires considerably less radio hardware.

Therefore, we consider that the defined requirements and limitations are close to the performance limits of the presented proposal, since the required precision may be difficult to obtain in practice. However, the proposal also allows the use of simpler and different implementation possibilities if less demanding requirements and limitations can be set. Furthermore, the developed analytical model and evaluation platform allow further study, both theoretical and experimental, of alternatives and improvements that might be proposed for the antenna system for OLFAR's ISL.

6.2 Recommendations

Even though the presented proposal covers several aspects of the antenna system, further work should still be performed to complete an optimized solution. A careful design of the individual antennas is fundamental to have a better idea of the antenna characteristics (for different types of antennas). Simulations with microwave design software can then be carried out to estimate the performance of the antenna system in space. Additionally, a custom design of an integrated RF-to-bits transceiver for the antenna system can give insight into its power requirements. Furthermore, it is also necessary to perform a study of the bandwidth required for the ISL, which should involve the bandwidth of the individual antennas, the proposed multiple access technique and an eventual frequency reuse plan. If the ISLs can no longer be considered narrowband, then the beamforming algorithm must be re-evaluated.

Besides this, other smaller optimizations and studies can be performed for the proposed inter-satellite links. An optimization of the adaptive clustering algorithm could balance better the bandwidth and power requirements between masters and slaves, relaxing the link budget. Different possibilities for DOA estimation and ranging techniques must also be studied in order to provide reliable and efficient localization capabilities. Moreover, the impact of errors in the estimation of the direction of arrival or the individual antenna radiation pattern could also be studied.

Finally, the experiments with the evaluation platform could be performed with higher precision, considering the coupling between the fields of the different antennas and using alternative support mechanisms. Additionally, the platform can also be improved with a digital signal processor (DSP) and even a field programmable gate array (FPGA) to provide higher baseband bandwidths. Experiments involving beamfoming in the transmitter, real-time operation and evaluation of the performance of the proposed coding and modulation schemes can be carried out in such an improved evaluation platform.

Bibliography

[1] K. G. Jansky, "Directional Studies of Atmospherics at High Frequencies," *Proceedings of the Institute of Radio Engineers*, vol. 20, no. 12, pp. 1920–1932, December 1932.

[2] K. I. Kellermann and I. I. K. Pauliny-Toth, "Extragalactic radio sources," *Proceedings of the IEEE*, vol. 61, no. 9, pp. 1174–1182, September 1973.

[3] G. F. Smoot, "Nobel Lecture: Cosmic microwave background radiation anisotropies: Their discovery and utilization," *Reviews of Modern Physics*, vol. 79, pp. 1349–1379, November 2007.

[4] B. F. Burke and F. Graham-Smith, *An Introduction to Radio Astronomy*, 3rd ed. Cambridge University Press, 2010.

[5] M. L. Kaiser and K. W. Weiler, "The Current Status of Low Frequency Radio Astronomy from Space," in *Radio Astronomy at Long Wavelengths*, ser. Geophysical Monograph Series, R. Stone, K. W. Weiler, M. Goldstein, and J. Bougeret, Eds., vol. 119. The American Geophysical Union, 2000, pp. 1–11.

[6] J. M. Payne, "Millimeter and submillimeter wavelength radio astronomy," *Proceedings of the IEEE*, vol. 77, no. 7, pp. 993 –1017, July 1989.

[7] J. P. Basart, J. O. Burns, B. K. Dennison, K. W. Weiler, N. E. Kassim, S. P. Castillo, and B. M. McCune, "Directions for space-based low frequency radio astronomy 1. System considerations," *Radio Science*, vol. 32, no. 1, pp. 251–263, January-February 1997.

[8] M. J. Bentum and A. J. Boonstra, "Low frequency astronomy - The challenge in a crowded RFI environment," in *XXXth URSI General Assembly and Scientific Symposium*, August 2011, pp. 1–4.

[9] Infrarred Processing and Analysis Center (IPAC) and National Aeronautics and Space Administration (NASA), "Infrared Windows," Infrared Processing and Analysis Center (IPAC) public web site. [Online]. Available: http://www.ipac.caltech.edu/outreach/Edu/Windows/irwindows.html

[10] J. Findlay, “Radio telescopes,” *IEEE Transactions on Antennas and Propagation*, vol. 12, no. 7, pp. 853–864, December 1964.

[11] S. W. Ellingson, “Antennas for the next generation of low-frequency radio telescopes,” *IEEE Transactions on Antennas and Propagation*, vol. 53, no. 8, pp. 2480–2489, August 2005.

[12] M. Ryle and A. Hewish, “The synthesis of large radio telescopes,” *Monthly Notices of the Royal Astronomical Society*, vol. 120, p. 220, 1960.

[13] G. W. Swenson, Jr. and N. C. Mathur, “The interferometer in radio astronomy,” *Proceedings of the IEEE*, vol. 56, no. 12, pp. 2114–2130, December 1968.

[14] A. S. Cohen, W. M. Lane, W. D. Cotton, N. E. Kassim, T. J. W. Lazio, R. A. Perley, J. J. Condon, and W. C. Erickson, “The VLA Low-Frequency Sky Survey,” *The Astronomical Journal*, vol. 134, no. 3, pp. 1245–1262, September 2007.

[15] G. Swarup, S. Ananthakrishnan, V. K. Kapahi, A. P. Rao, C. R. Subrahmanya, and V. K. Kulkarni, “The Giant Metre-wave Radio Telescope,” *Current Science*, vol. 60, no. 2, pp. 95–105, January 1991.

[16] A. W. Gunst and M. J. Bentum, “The LOFAR phased array telescope system,” in *IEEE International Symposium on Phased Array Systems and Technology (ARRAY)*, October 2010, pp. 632 –639.

[17] J. K. Alexander, M. L. Kaiser, J. C. Novaco, F. R. Grena, and R. R. Weber, “Scientific instrumentation of the Radio-Astronomy-Explorer-2 satellite,” *Astronomy and Astrophysics*, vol. 40, no. 4, pp. 365–371, May 1975.

[18] M. J. Bentum, A. J. Boonstra, and W. Baan, “Space-based ultra-long wavelength radio astronomy - an overview of today’s initiatives,” in *XXXth URSI General Assembly and Scientific Symposium*, August 2011, pp. 1–4.

[19] S. Jester and H. Falcke, “Science with a lunar low-frequency array: From the dark ages of the Universe to nearby exoplanets,” *New Astronomy Reviews*, vol. 53, no. 1-2, pp. 1–26, 2009.

[20] J. P. Basart, J. O. Burns, B. K. Dennison, K. W. Weiler, N. E. Kassim, S. P. Castillo, and B. M. McCune, “Directions for space-based low frequency radio astronomy 2. Telescopes,” *Radio Science*, vol. 32, no. 1, pp. 265–275, January-February 1997.

[21] M. J. Bentum, C. J. M. Verhoeven, A. J. Boonstra, E. K. A. Gill, and A. J. van der Veen, “A novel astronomical application for formation flying small satellites,”

in *60th International Astronautical Congress (IAC)*. International Astronautical Federation (IAF), October 2009, pp. 1–8.

[22] C. J. M. Verhoeven, M. J. Bentum, G. L. E. Monna, J. Rotteveel, and J. Guo, “On the origin of satellite swarms,” *Acta Astronautica*, vol. 68, no. 7-8, pp. 1392–1395, April-May 2011.

[23] S. Engelen, E. K. A. Gill, and C. J. M. Verhoeven, “On the reliability of spacecraft swarms,” in *Small Satellites and Services Symposium (4S)*, May-June 2012.

[24] ——, “Systems engineering challenges for satellite swarms,” *IEEE Aerospace Conference*, pp. 1–8, March 2011.

[25] R. T. Rajan, S. Engelen, M. J. Bentum, and C. J. M. Verhoeven, “Orbiting Low Frequency Array for Radio astronomy,” in *IEEE Aerospace Conference*, March 2011, pp. 1–11.

[26] M. Werner, A. Jahn, E. Lutz, and A. Bottcher, “Analysis of system parameters for LEO/ICO-satellite communication networks,” *IEEE Journal on Selected Areas in Communications*, vol. 13, no. 2, pp. 371–381, February 1995.

[27] H. Keller and H. Salzwedel, “Link strategy for the mobile satellite system Iridium,” in *46th IEEE Vehicular Technology Conference: ’Mobile Technology for the Human Race’*, vol. 2, April-May 1996, pp. 1220–1224.

[28] S. R. Pratt, R. A. Raines, C. E. Fossa, and M. A. Temple, “An operational and performance overview of the IRIDIUM low earth orbit satellite system,” *IEEE Communications Surveys Tutorials*, vol. 2, no. 2, pp. 2–10, Second Quarter 1999.

[29] A. Budianu, T. Willink Castro, A. Meijerink, and M. J. Bentum, “Communication schemes for OLFAR’s inter-satellite links,” in *63rd International Astronautical Congress (IAC)*. International Astronautical Federation (IAF), October 2012.

[30] A. Budianu, R. T. Rajan, S. Engelen, A. Meijerink, C. J. M. Verhoeven, and M. J. Bentum, “OLFAR: Adaptive topology for satellite swarms,” in *62nd International Astronautical Congress (IAC)*. International Astronautical Federation (IAF), October 2011, pp. 1–9.

[31] A. F. Molisch, *Wireless Communications*, ser. Wiley - IEEE. John Wiley & Sons, 2011.

[32] California Polytechnic Institute, *CubeSat Design Specification*, August 2009, Revision 12. [Online]. Available: http://www.cubesat.org/images/developers/cds_rev12.pdf

[33] S. Notani and S. Bhattacharya, “Flexible electrical power system controller design and battery integration for 1U to 12U CubeSats,” in *IEEE Energy Conversion Congress and Exposition (ECCE)*, September 2011, pp. 3633–3640.

[34] L. C. Godara, “Application of antenna arrays to mobile communications. II. Beam-forming and direction-of-arrival considerations,” *Proceedings of the IEEE*, vol. 85, no. 8, pp. 1195–1245, August 1997.

[35] C. A. Balanis, *Antenna Theory: Analysis and Design*, 3rd ed. John Wiley & Sons, 2005.

[36] M. Koubeissi, Y. Abdallah, E. Arnaud, M. Thevenot, T. Monediere, T. Koleck, and E. Peragin, “WideBand WideAngle circular polarization of a multilayer patch antenna,” in *Proceedings of the Fourth European Conference on Antennas and Propagation (EuCAP)*, April 2010, pp. 1–4.

[37] V. L. Pisacane, *Fundamentals of Space Systems*, 2nd ed. Oxford University Press, 2005.

[38] Taoglas Antenna Solutions, *WLP.2450.25.4.A.02 2450MHz Patch Antenna Specification*. [Online]. Available: http://www.taoglas.com/images/product_images/original_images/WLP.2450.25.4.A.02%202450MHz%20Ceramic%20Patch%20100310.pdf

[39] W. C. van Etten, *Introduction to Random Signals and Noise*, 1st ed. John Wiley & Sons, 2005.

[40] P. L. Richards, “Cosmic Microwave Background Experiments - Past, Present and Future,” in *Joint 32nd International Conference on Infrared and Millimeter Waves and 15th International Conference on Terahertz Electronics (IRMMW-THz)*, September 2007, pp. 12–15.

Appendix A

Derivation of the receiver noise parameters

A radio receiver's performance is usually characterized by its figure of merit G/T or a noise figure NF along with a noise floor N. These parameters are normally developed for conditions of Earth-bound communications, specially a standard temperature of 290 K [39]. However, using the appropriate expressions, they can be defined to suit the scenario of an inter-satellite link.

A.1 Noisy receiver model

We consider a noisy receiver model in which the elements that involve noise contributions are the antenna, its (lossy) feed, the LNA, the (also lossy) line to the downconverter and the downconverter. Other noisy elements that may be present in a real receiver (like baluns and filters) are considered as part of the modelled elements. Figure A.1 shows the noisy receiver model and the configuration of its different elements.

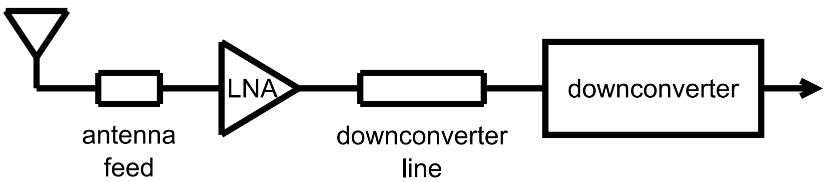

Figure A.1: Noisy receiver model.

A.1.1 Individual elements equivalent model

To model the noise contributions of each element, we consider their (power) gain G_{elem} and effective noise temperature T_{elem}. Moreover, we assume that the noise bandwidth of the receiver $W_{\rm N}$ is the (cluster-head) channel badwidth discussed in Section 2.2. Then, each element can be represented as an ideal gain block and an equivalent noise source at its input [39]. The receiver antenna, however, is modelled as an equivalent noise source with no gain block, since it represents the initial noise source of the receiver [39]. Figure A.2 shows the receiver model with the equivalent blocks of its individual elements.

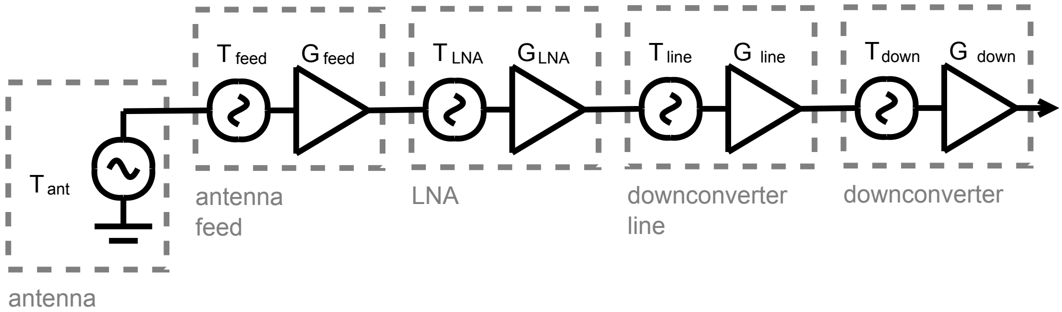

Figure A.2: Receiver model with equivalent blocks of its individual elements.

The antenna noise temperature is mostly given by the background noise radiation it picks up. For our scenario, this will mainly be cosmic microwave background radiation [40] (at about 3 K), with some contributions from the Sun, the Moon and the Earth. We consider an antenna noise temperature of approximately 10 K to account for these celestial noise contributions.

The noise temperature of the different passive elements is determined by their loss $L_{\rm elem} = 1/G_{\rm elem}$ and the ambient temperature $T_{\rm amb}$ [39]:

$$T_{\rm passive} = (L_{\rm elem} - 1)\, T_{\rm amb}\,. \tag{A.1}$$

For the active elements, the effective noise temperature considers several different noise contributions [39]. To model this, we use their standard noise figure specification $NF_{\rm active}$, from which the effective noise temperature can be calculated [39]:

$$T_{\rm active} = (F_{\rm active} - 1)\, 290\,, \tag{A.2}$$

where $F_{\rm active} = 10^{NF_{\rm active}/10}$ is the element's standard noise factor.

A.1.2 Equivalent model

Because in the link budget from Section 2.5 we considered the gain of the receiving antenna and the losses of its feed, the received signal-to-noise ratio (SNR) is calculated *after* the antenna feed. Therefore, the receiver's input noise is given by the antenna and its feed, while its noise contribution is given by the remaining components (i.e. LNA, the downconverter and its line).

Then, using the individual elements' equivalent blocks, we obtained a simplified model that consists in an effective source noise temperature of the antenna and its feed $T_{\mathrm{R,s}}$ and the receiver's equivalent input noise temperature $T_{\mathrm{R,e}}$. Figure A.3 shows the equivalent receiver model.

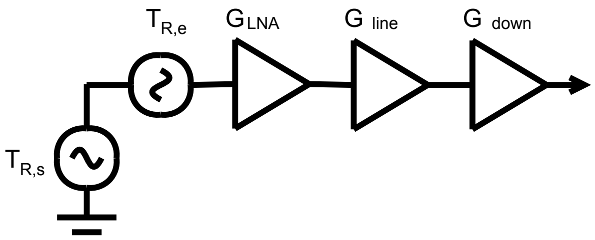

Figure A.3: Receiver model with equivalent noise sources.

Then, the equivalent noise temperature of the two noise sources can be obtained using Friis formula [39]:

$$T_{\mathrm{R,s}} = (T_{\mathrm{ant}} + T_{\mathrm{feed}})\ G_{\mathrm{feed}}\ , \tag{A.3}$$

$$T_{\mathrm{R,e}} = T_{\mathrm{LNA}} + \frac{T_{\mathrm{line}}}{G_{\mathrm{LNA}}} + \frac{T_{\mathrm{downconv}}}{G_{\mathrm{LNA}}\, G_{\mathrm{line}}}\ . \tag{A.4}$$

A.2 Receiver noise parameters

A.2.1 Figure of merit

The receiver's figure of merit relates its equivalent gain $G_{\mathrm{R,equiv}} = G_{\mathrm{ant}}\, G_{\mathrm{feed}}$ and its *system* noise temperature $T_{\mathrm{R,sys}} = T_{\mathrm{R,s}} + T_{\mathrm{R,e}}$ [39], and is expressed in dB/K:

$$G/T = 10 \log \left(\frac{G_{\mathrm{R,equiv}}}{T_{\mathrm{R,sys}}} \right)\ . \tag{A.5}$$

A.2.2 Noise figure and noise floor

The receiver's noise floor is given by its input noise temperature and noise bandwidth [39]:

$$N = k\, T_{\mathrm{R,s}}\, W_{\mathrm{N}}\ , \tag{A.6}$$

where $k = 1.38 \times 10^{-23}$ J/K is the Boltzmann constant.

The receiver's (operational) noise figure is the ratio in dB of its effective and input noise temperatures [39]:

$$NF = 10 \log \left(1 + \frac{T_{\mathrm{R,e}}}{T_{\mathrm{R,s}}} \right)\ . \tag{A.7}$$

A.3 Results

A.3.1 Antenna system proposal

For the transceiver proposed for the antenna system for OLFAR's ISL, suitable noise specifications of the different elements of the receiver are shown in Table A.1. For this proposal, we assume that each satellite is capable of ensuring an ambient temperature for its electronics of at most 80 $^{\circ}$C (353 K).

Table A.1: Proposed receiver noise characteristics.

Device	Gain		Noise factor	Noise figure (dB)	Noise temp. (K)
	linear	dB			
Antenna	3.16	5	-	-	10
Antenna feed	0.9	-0.46	-	-	39.22
LNA	100	20	1.2	0.8	71.4
Downconverter line	0.95	-0.22	-	-	17.65
Downconverter	100	20	3.98	6	1052

Then, the resulting receiver noise parameters for these specifications are:

- figure of merit G/T of -16.49 dB/K;
- noise figure NF of 4.57 dB;
- noise floor N of -107.1 dBm.

A.3.2 Evaluation platform

The noise parameters of the different elements of the receiver in the evaluation platform are shown in Table A.2. An ambient temperature of 290 K and a bandwidth of 50 kHz were considered in this case, matching the experiment settings presented in Section 5.2.

For these specifications, the resulting receiver noise parameters are:

- figure of merit G/T of -33.7 dB/K;
- noise figure NF of 1.88 dB;
- noise floor N of -127.3 dBm.

Table A.2: Evaluation platform receiver noise characteristics.

Device	**Gain**		**Noise factor**	**Noise figure (dB)**	**Noise temp. (K)**
	linear	**dB**			
Antenna	2.51	4	-	-	10
Antenna feed	0.07	-11.5	-	-	3806
LNA	100	20	1.2	0.8	58.66
Downconverter line	0.5	-3	-	-	145
Downconverter	4467	36.5	15.85	12	4306